PLOS PATHOGENS

RESEARCH ARTICLE

Killing from the inside: Intracellular role of T3SS in the fate of *Pseudomonas aeruginosa* within macrophages revealed by *mgtC* and *oprF* mutants

Preeti Garai[1], Laurence Berry[1☯], Malika Moussouni[1☯], Sophie Bleves[2], Anne-Béatrice Blanc-Potard[1]*

1 Laboratoire de Dynamique des Interactions Membranaires Normales et Pathologiques, Université de Montpellier, CNRS-UMR5235, Montpellier, France, **2** LISM, Institut de Microbiologie de la Méditerranée, CNRS & Aix-Marseille Univ, Marseille, France

☯ These authors contributed equally to this work.
* anne.blanc-potard@umontpellier.fr

OPEN ACCESS

Citation: Garai P, Berry L, Moussouni M, Bleves S, Blanc-Potard A-B (2019) Killing from the inside: Intracellular role of T3SS in the fate of *Pseudomonas aeruginosa* within macrophages revealed by *mgtC* and *oprF* mutants. PLoS Pathog 15(6): e1007812. https://doi.org/10.1371/journal.ppat.1007812

Editor: Joan Mecsas, Tufts University, UNITED STATES

Received: January 18, 2019

Accepted: May 2, 2019

Published: June 20, 2019

Data Availability Statement: All relevant data are within the manuscript and its Supporting Information files.

Funding: This work is supported by Vaincre La Mucoviscidose (http://www.vaincrelamuco.org/) (RF20150501356/1/1/47 and RIF20170502042) and Association Gregory Lemarchal (https://association-gregorylemarchal.org/). PG is supported by the Association Méditerranée Infection (http://www.mediterranee-infection.com/

Abstract

While considered solely an extracellular pathogen, increasing evidence indicates that *Pseudomonas aeruginosa* encounters intracellular environment in diverse mammalian cell types, including macrophages. In the present study, we have deciphered the intramacrophage fate of wild-type *P. aeruginosa* PAO1 strain by live and electron microscopy. *P. aeruginosa* first resided in phagosomal vacuoles and subsequently could be detected in the cytoplasm, indicating phagosomal escape of the pathogen, a finding also supported by vacuolar rupture assay. The intracellular bacteria could eventually induce cell lysis, both in a macrophage cell line and primary human macrophages. Two bacterial factors, MgtC and OprF, recently identified to be important for survival of *P. aeruginosa* in macrophages, were found to be involved in bacterial escape from the phagosome as well as in cell lysis caused by intracellular bacteria. Strikingly, type III secretion system (T3SS) genes of *P. aeruginosa* were down-regulated within macrophages in both *mgtC* and *oprF* mutants. Concordantly, cyclic di-GMP (c-di-GMP) level was increased in both mutants, providing a clue for negative regulation of T3SS inside macrophages. Consistent with the phenotypes and gene expression pattern of *mgtC* and *oprF* mutants, a T3SS mutant (Δ*pscN*) exhibited defect in phagosomal escape and macrophage lysis driven by internalized bacteria. Importantly, these effects appeared to be largely dependent on the ExoS effector, in contrast with the known T3SS-dependent, but ExoS independent, cytotoxicity caused by extracellular *P. aeruginosa* towards macrophages. Moreover, this macrophage damage caused by intracellular *P. aeruginosa* was found to be dependent on GTPase Activating Protein (GAP) domain of ExoS. Hence, our work highlights T3SS and ExoS, whose expression is modulated by MgtC and OprF, as key players in the intramacrophage life of *P. aeruginosa* which allow internalized bacteria to lyse macrophages.

). MM is supported by Vaincre La Mucoviscidose (RIF20170502042). The funders had no role in study design, data collection and analysis, decision to publish, or preparation of the manuscript.

Competing interests: The authors have declared that no competing interests exist.

Author summary

The ability of professional phagocytes to ingest and kill microorganisms is central to host defense and *Pseudomonas aeruginosa* has developed mechanisms to avoid being killed by phagocytes. While considered an extracellular pathogen, *P. aeruginosa* has been reported to be engulfed by macrophages in animal models. Here, we visualized the fate of *P. aeruginosa* within cultured macrophages, revealing macrophage lysis driven by intracellular *P. aeruginosa*. Two bacterial factors, MgtC and OprF, recently discovered to be involved in the intramacrophage survival of *P. aeruginosa*, appeared to play a role in this cytotoxicity caused by intracellular bacteria. We provided evidence that type III secretion system (T3SS) gene expression is lowered intracellularly in *mgtC* and *oprF* mutants. We further showed that intramacrophage *P. aeruginosa* uses its T3SS, specifically the ExoS effector, to promote phagosomal escape and cell lysis. We thus describe a transient intramacrophage stage of *P. aeruginosa* that could contribute to bacterial dissemination.

Introduction

Pathogenic bacteria are commonly classified as intracellular or extracellular pathogens [1]. Intracellular bacterial pathogens, such as *Mycobacterium tuberculosis* or *Salmonella enterica*, can replicate within host cells, including macrophages. In contrast, extracellular pathogens, such as *Yersinia* spp., *Staphylococcus aureus*, *Pseudomonas aeruginosa* or streptococci, avoid phagocytosis or exhibit cytotoxicity towards phagocytic cells, to promote their extracellular multiplication. However, recent data have emphasized that several extracellular pathogens can enter host cells *in vivo*, resulting in a phase of intracellular residence, which can be of importance in addition to the typical extracellular infection. For example, although *Yersinia* spp. subvert the functions of phagocytes from the outside, these bacteria also subvert macrophage functions within the cell [2]. Once considered an extracellular pathogen, it is now established that *S. aureus* can survive within many mammalian cell types including macrophages [3,4] and the intramacrophage fate of *S. aureus* has been deciphered [5,6]. Moreover, an intracellular phase within splenic macrophages has been recently shown to play a crucial role in initiating dissemination of *Streptococcus pneumoniae*, providing a divergence from the dogma that considered this bacterial pathogen a classical example of extracellular pathogens [7].

The environmental bacterium and opportunistic human pathogen *P. aeruginosa* is responsible for a variety of acute infections and is a major cause of mortality in chronically infected cystic fibrosis (CF) patients. The chronic infection of *P. aeruginosa* and its resistance to treatment is largely due to its ability to form biofilms, which relies on the production of exopolysaccharides (EPS), whereas the type III secretion system (T3SS) is reported to play a key role in the pathogenesis of acute *P. aeruginosa* infections [8]. Four T3SS effectors (ExoU, ExoS, ExoT, ExoY) have been identified so far, ExoS being nearly always mutually exclusive with the potent cytotoxin ExoU and more prevalent than ExoU [9–11]. ExoS has a dual function as it contains a GTPase activating protein (GAP) domain as well as an ADP ribosyltransferase (ADPRT) domain [10]. An intracellular step in airway epithelial cells has been proposed to occur before the formation of biofilm during the acute phase of infection [12,13] and the intracellular stage of *P. aeruginosa* within cultured epithelial cells has been fairly studied [14–16]. The principle that *P. aeruginosa* is not exclusively an extracellular pathogen has been convincingly established by the recent use of advanced imaging methods to track bacteria within epithelial cells [17]. The T3SS, more specifically its effector ExoS, has been implicated in the formation of membrane blebs-niche and avoidance of acidified compartments to allow bacterial

multiplication within epithelial cells [17–19]. Concordantly, T3SS genes were recently shown to be expressed in *P. aeruginosa* internalized in epithelial cells [17]. Regarding the interaction with macrophages, *P. aeruginosa* has developed mechanisms to avoid phagocytosis [20]. However, *P. aeruginosa* has been shown to be phagocytosed by macrophages in an acute model of infection in zebrafish embryos [21,22] and has been reported to be engulfed by alveolar macrophages in the lungs of mice early after pulmonary infection [23], suggesting that *P. aeruginosa* may need strategies to escape macrophage killing. Although *P. aeruginosa* has been localized within cultured macrophages during gentamicin protection assays [24–26], the intramacrophage fate of the bacteria has not been characterized and bacterial factors involved in this step remain largely unexplored.

Bacterial survival in a particular niche requires the development of an adaptive response, generally mediated by regulation of the bacterial genes involved in physiological adaptation to the microenvironment. The identification of mutants lacking the ability to survive within macrophages and the study of *P. aeruginosa* gene expression inside macrophages is critical to determine bacterial players in this step. We have previously uncovered MgtC as a bacterial factor involved in the intramacrophage survival of *P. aeruginosa* [25,27]. In agreement with this intramacrophage role, expression of *Pseudomonas mgtC* (PA4635) gene is induced when the bacteria reside inside macrophages [25]. MgtC is known to promote intramacrophage growth in several classical intracellular bacteria, including *Salmonella typhimurium* where it inhibits bacterial ATP synthase and represses cellulose production [28–30], and is considered as a clue to reveal bacterial pathogens adapted to an intramacrophage stage [30,31]. In addition, a recent study has implicated the outer membrane protein OprF in the ability of otopathogenic *P. aeruginosa* strains to survive inside macrophages [26]. OprF is an outer membrane porin that can modulate the production of various virulence factors of *P. aeruginosa* [32,33].

In the present study, we investigated the fate of *P. aeruginosa* within macrophages using wild-type PAO1 strain, which lacks ExoU, along with isogenic *mgtC* and *oprF* mutants. We also explored, for the first time, the regulation of T3SS genes when *P. aeruginosa* resides inside macrophages. The T3SS and ExoS effector, whose expression was found to be modulated by MgtC and OprF intracellularly, were seemingly involved in this intracellular stage, playing a role in vacuolar escape and cell lysis caused by intracellular bacteria.

Results

Intracellular *P. aeruginosa* can promote macrophage lysis

We previously visualized fluorescent *P. aeruginosa* residing within fixed macrophages [25]. To investigate the fate of *P. aeruginosa* after phagocytosis in a dynamic way, we monitored macrophages infected with fluorescent bacteria using time-lapse live microscopy. J774 macrophages were infected with wild-type PAO1 strain expressing GFP grown exponentially in LB medium (Multiplicity of infection or MOI = 10). After 25 minutes of phagocytosis, several washes were performed to remove non-internalized bacteria and gentamicin was added to kill the remaining extracellular bacteria. Microscopic observation of infected macrophages up to 3 hours showed cell lysis with increasing time (Fig 1), starting between 1.5 and 2 hours post-phagocytosis, which can be attributed to intracellular bacteria as gentamicin was retained throughout the experiment. No lysis of uninfected cells present in the same field was observed (Fig 1 and S1 Fig), as expected from an event due to intracellular bacteria rather than extracellular bacteria. The cell lysis appeared to take place within a rapid time frame of few seconds, as shown by the movie (S1 Movie), after which the bacteria seemed to be released from the host cell. We also infected human monocyte-derived macrophages (HMDMs) with GFP producing PAO1 strain under similar conditions and found lysed infected cells after 2 hours of phagocytosis (S2

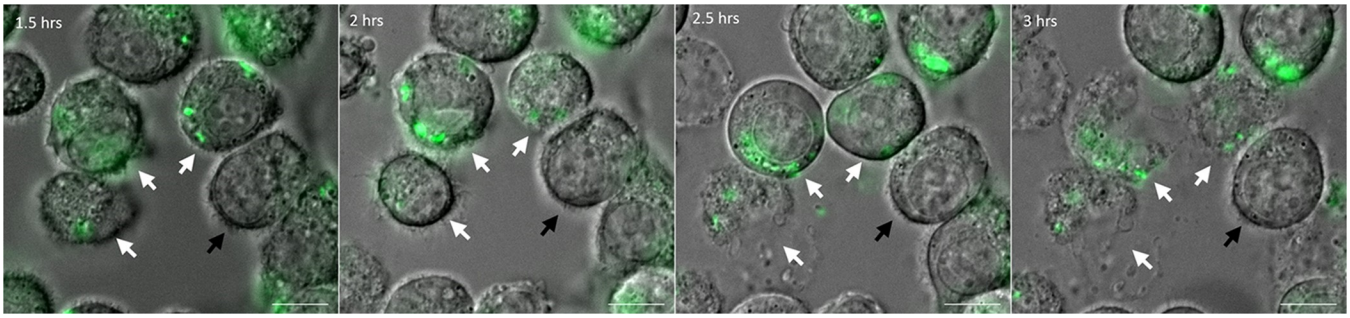

Fig 1. Live imaging of macrophages infected with *P. aeruginosa*. J774 macrophages were infected with PAO1 wild-type (WT) strain expressing GFP. Time lapse imaging was started at 1.5 hrs post-phagocytosis. Cells were maintained in DMEM supplemented with gentamicin at 37˚C and 5% CO_2 throughout imaging. White arrows point at the cells that harbor intracellular bacteria and undergo lysis between 1.5 hrs and 3 hrs post-phagocytosis. Black arrow shows an uninfected and unlysed cell. Scale bar is equivalent to 10 μm.

https://doi.org/10.1371/journal.ppat.1007812.g001

Fig). Hence, the phenomenon of lysis of macrophages by intracellular PAO1 is not restricted to J774 murine cell line, but is extendable to primary human macrophages.

We further examined intracellular *P. aeruginosa* within macrophages in more detail using transmission electron microscopy (TEM). J774 macrophages infected with wild-type PAO1 strain, were subjected to fixation at early time post-infection (30 min after phagocytosis) or at later time of infection (3 hrs after phagocytosis). After phagocytosis, *P. aeruginosa* was present in membrane bound vacuoles inside macrophages (Fig 2A). At a later time point, some bacteria could be found in the cytoplasm with no surrounding membrane, suggesting disruption of the vacuole membrane (Fig 2B). The infected macrophage was damaged, displaying highly condensed chromatin and membrane blebbing, and lacking pseudopodia. Healthy infected cells were also observed, where bacteria were mostly found in vacuoles partially or totally filled with heterogeneous electron dense material, suggesting that the vacuole has fused with lysosomes (Fig 2C). To confirm this, we examined the association between fluorescent PAO1 bacteria and the LysoTracker probe during infection using fixed macrophages. Bacteria colocalizing with LysoTracker could be visualized (S3 Fig), thereby corroborating the TEM observation of fusion of vacuoles with lysosomes and the localization of bacteria in acidified compartment.

TEM analyses allowed us to conclude that wild-type PAO1 strain has the ability to reside within vacuoles and possibly escape from the phagosome into the cytoplasm, and promote cell damage. A rapid cell lysis event caused by intracellular *P. aeruginosa* visualized by live microscopy revealed that phagocytosed bacteria can escape from macrophage through cell lysis.

Intracellular *mgtC* and *oprF* mutants are compromised in cell lysis

Our previous results based on gentamicin protection assay on J774 infected macrophages and counting of colony forming units (CFU) indicated that *mgtC* mutant (generated in the PAO1 background) survived to a lesser extent than the wild-type strain [25]. More recently, an *oprF* mutant of an otopathogenic strain of *P. aeruginosa* was also found to be defective in intracellular survival in mouse bone marrow macrophages based on gentamicin protection assay [26]. To analyze the phenotypes of *oprF* mutant in the PAO1 background towards J774 macrophages and compare that with *mgtC* mutant, we used here a previously described *oprF* mutant generated in PAO1 strain [25,34].

Based on the finding that intracellular *P. aeruginosa* can cause macrophage lysis, we developed a suitable assay using fluorescent microscopic analysis to quantify cell damage caused by intracellular bacteria. Macrophages were infected with fluorescent bacteria, treated with

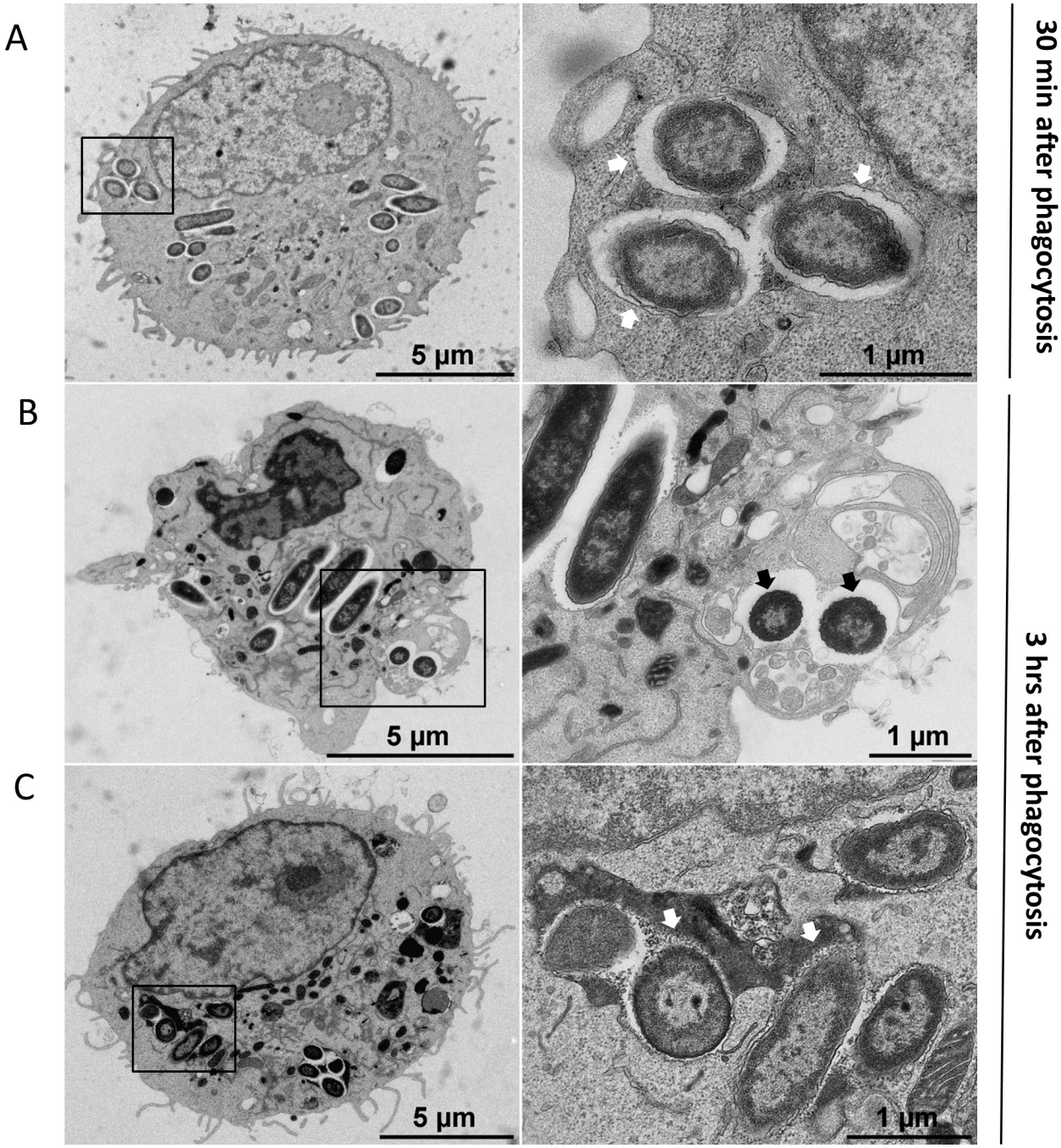

Fig 2. Transmission electron micrographs (TEM) of *P. aeruginosa* within macrophages. J774 macrophages were infected with *P. aeruginosa* for 30 min (A) or 3 hrs (B and C) and subjected to TEM (left panels). Black rectangles show intracellular bacteria that are shown at higher magnification in the right panels. A. At early time after phagocytosis, most of bacteria were found inside membrane bound vacuoles (white arrows). B. At later time, some bacteria can be observed in the cytoplasm with no surrounding membrane suggesting disruption of the vacuole membrane (black arrows). The infected macrophage in panel B shows an abnormal morphology, with highly condensed chromatin and membrane blebbing, but no pseudopodia. C. At later time, bacteria can also be found in vacuole partially or totally filled with heterogeneous electron dense material (white arrows), suggesting that the vacuole has fused with lysosomes. The infected macrophage shown in panel C appears normal.

https://doi.org/10.1371/journal.ppat.1007812.g002

gentamicin for 2 hours after phagocytosis, fixed and stained with phalloidin-TRITC to label F-actin and visualize macrophage morphology. A clear cortical red labeling was seen in most

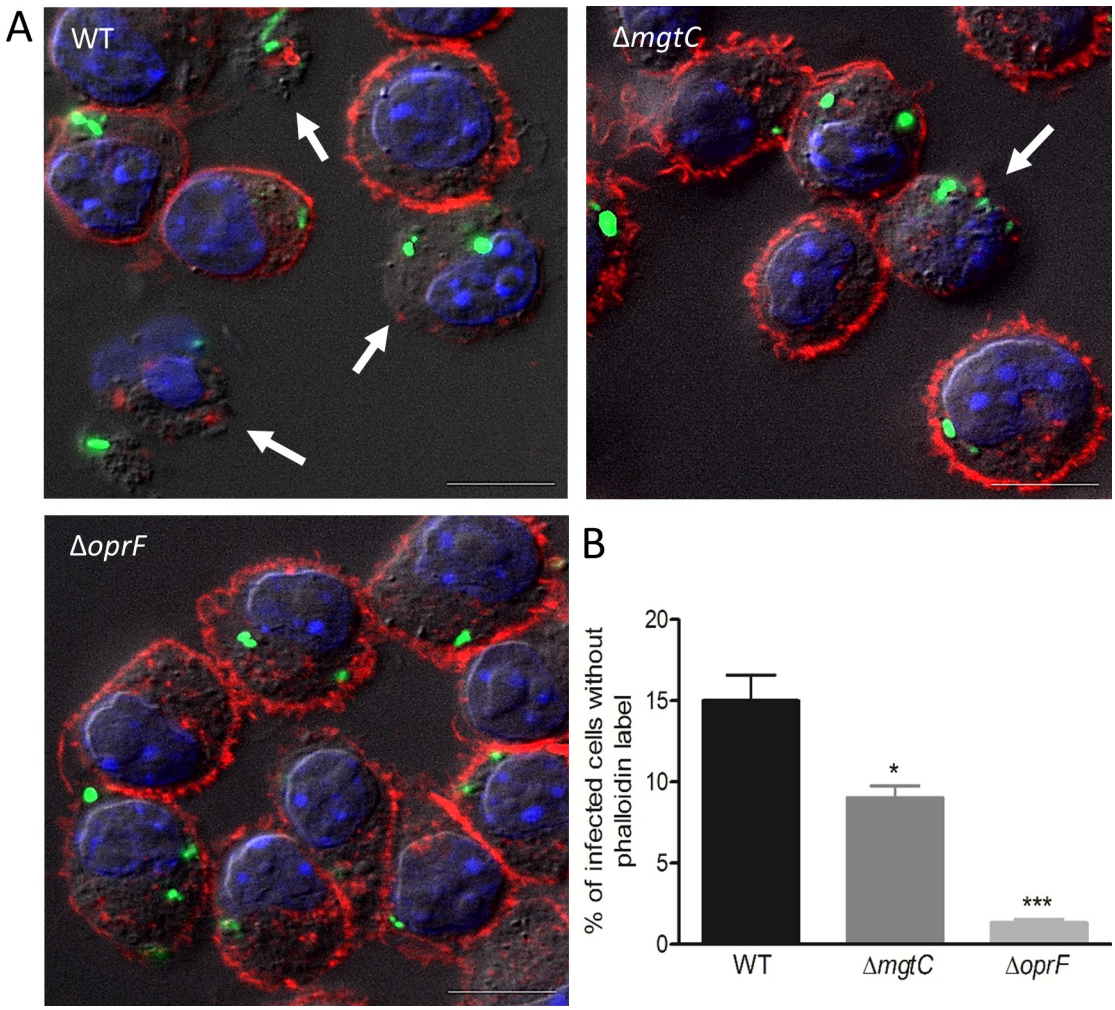

Fig 3. Visualization (A) and quantification (B) of lysed infected cells upon phalloidin labeling. GFP expressing PAO1 WT, Δ*mgtC* and Δ*oprF* strains were used for infecting J774 macrophages. Gentamicin was added after phagocytosis and cells were fixed at 2 hrs post-phagocytosis, stained with phalloidin and imaged with fluorescent microscope. DAPI was used to stain the nucleus. Cells that have intracellular bacteria, but lack the phalloidin cortical label were considered as lysed by intracellular bacteria (shown by arrows). Scale bar is equivalent to 10 μm. After imaging, infected cells were counted and percentage of lysed cells with intracellular bacteria out of total number of cells was plotted for each strain. Error bars correspond to standard errors from three independent experiments. At least 200 cells were counted per strain. The asterisks indicate *P* values (One way ANOVA, where all strains were compared to WT using Dunnett's multiple comparison post-test, $^{*}P < 0.05$ and $^{***}P < 0.001$), showing statistical significance with respect to WT.

https://doi.org/10.1371/journal.ppat.1007812.g003

cells, which is indicative of the plasma membrane-associated cortical actin. Few infected cells appeared lysed due to the loss of cortical actin staining (Fig 3A), which agrees with the observation of lysed macrophages in time lapse fluorescence microscopy (Fig 1). The loss of cortical actin staining was found to be due to internalized bacteria because upon arresting phagocytosis, by treating macrophages with cytochalasin D, bacteria were not internalized and loss of cortical actin staining was not observed (S4 Fig). Hence, any delayed effect of extracellular bacteria occurring before gentamicin treatment or a contribution of extracellular bacteria that would resist gentamicin treatment can be ruled out. Quantification of the number of cells without phalloidin labelling showed highest value for cells infected with wild-type strain, intermediate with *mgtC* mutant and lowest with *oprF* mutant (Fig 3B). Thus, both intracellular *mgtC* and *oprF* mutants appeared compromised for cell lysis. This feature is not linked to a

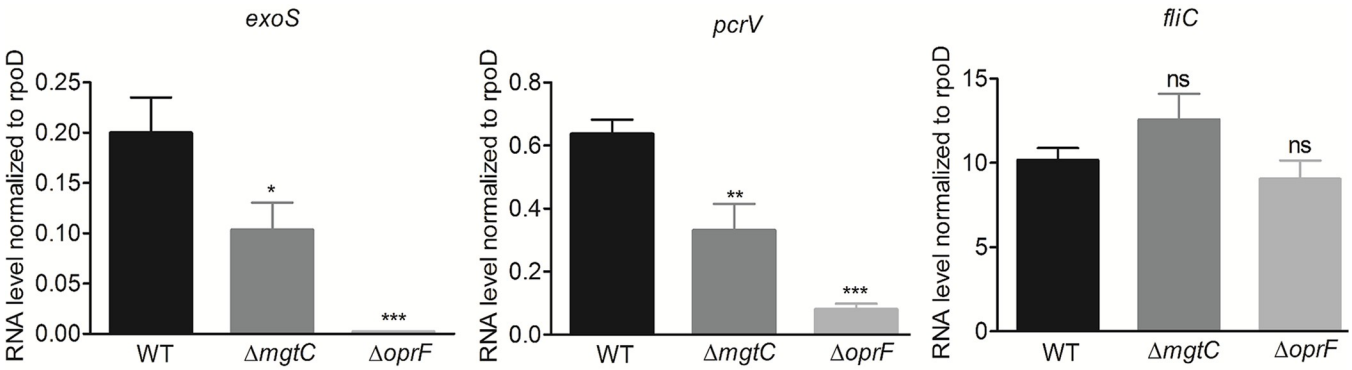

Fig 4. Expression of T3SS genes in *P. aeruginosa* strains residing in J774 macrophages. J774 macrophages were infected with PAO1 WT, Δ*mgtC* and Δ*oprF* strains. After phagocytosis, cells were maintained in DMEM supplemented with gentamicin. RNA was extracted from bacteria isolated from infected macrophages 1 hr after phagocytosis. The level of *exoS*, *pcrV* and *fliC* transcripts relative to those of the house-keeping gene *rpoD* was measured by qRT-PCR and plotted on the Y-axis. Error bars correspond to standard errors from at least three independent experiments. The asterisks indicate *P* values (One way ANOVA, where all strains were compared to WT using Dunnett's multiple comparison post-test, $^{*}P < 0.05$, $^{**}P < 0.01$, $^{***}P < 0.001$ and ns = $P > 0.05$ or non-significant), showing statistical significance with respect to WT.

https://doi.org/10.1371/journal.ppat.1007812.g004

lower internalization rate of the mutant strains, because *mgtC* mutant is known to be more phagocytosed than wild-type strain [25] and a similar trend was found for *oprF* mutant (not shown). Since T3SS has been involved in the intracellular life of *P. aeruginosa* in other cell types [17], we next monitored the expression of T3SS genes during the residence of bacteria within macrophages.

Down-regulation of T3SS gene expression in *mgtC* and *oprF* mutants inside macrophages

The *P. aeruginosa oprF* mutant was reported to be defective in the secretion of T3SS effectors in liquid culture and in the production of PcrV, the T3SS needle tip protein [32,34], but the effect of OprF on transcription of T3SS genes has not been tested so far. We thus investigated the expression of the effector gene *exoS* along with the gene *pcrV* in *oprF* mutant strain in comparison to wild-type strain upon macrophage infection. As a control, we tested flagellin coding gene *fliC*, which is not part of the T3SS regulon, but was proposed to be secreted by the T3SS [35]. Expression of both *pcrV* and *exoS* genes was found to be remarkably reduced in the *oprF* mutant (Fig 4). Strikingly, the *mgtC* mutant also exhibited significantly reduced expression of these two T3SS genes (Fig 4), although to a lesser extent than the *oprF* mutant, indicating an unexpected interplay between MgtC and T3SS. On the other hand, *fliC* expression was not altered in both mutants.

Since we observed a decreased transcriptional level of T3SS genes in the *oprF* mutant, we further examined the link between intramacrophage expression of T3SS and cell lysis in this mutant. A recombinant plasmid allowing IPTG-inducible overproduction of ExsA, a master transcriptional activator of T3SS genes [36], was introduced in the *oprF* mutant. Upon induction of *exsA* expression with 0.01 mM IPTG, *oprF* mutant promoted macrophage lysis like the wild-type strain (S5 Fig), supporting a model whereby the effect of OprF is the result of its positive regulatory effect on T3SS expression.

To address the mechanism behind the downregulation of transcription of T3SS in *oprF* and *mgtC* mutant strains, we evaluated the level of the second messenger c-di-GMP, as it is known to participate in T3SS repression in *P. aeruginosa* [37]. The *oprF* mutant was already reported to have high production of c-di-GMP in liquid culture [34]. We used a fluorescence-based

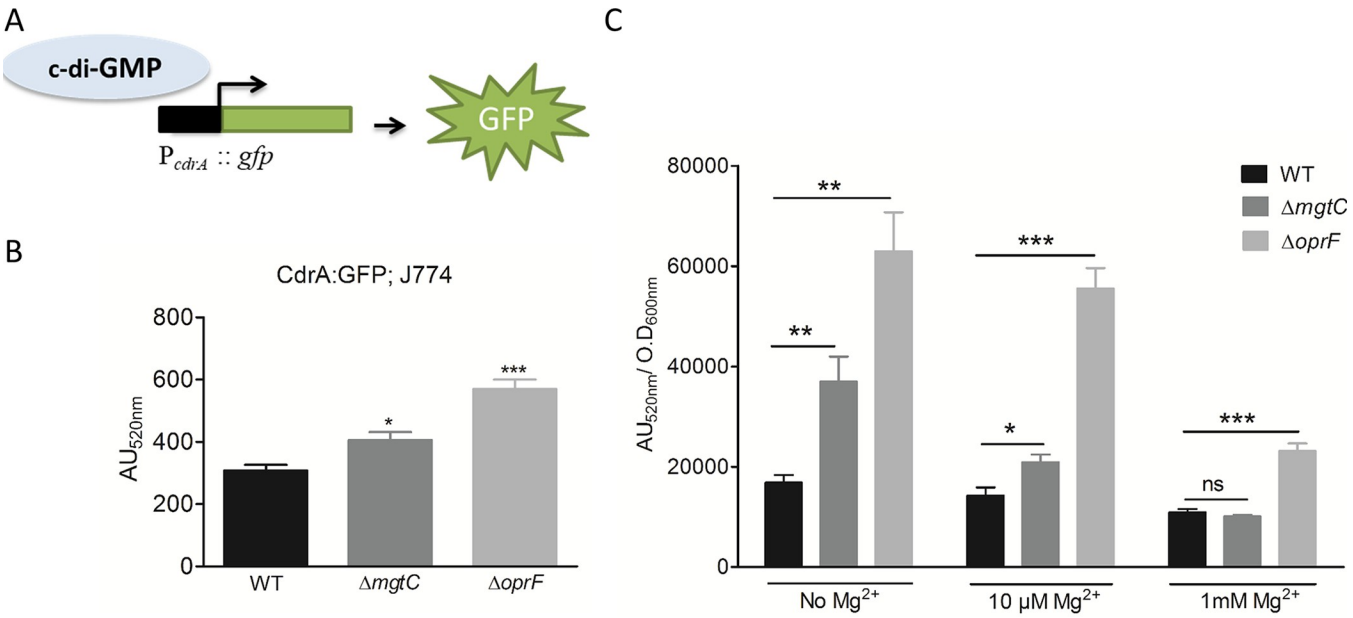

Fig 5. Measurement of c-di-GMP level in Δ*mgtC* and Δ*oprF* mutants. PAO1 WT, Δ*mgtC* and Δ*oprF* harboring reporter plasmid pCdrA::*gfp*, which expresses GFP under the control of the promoter of c-di-GMP responsive gene *cdrA* (A), were used to infect J774 cells and fluorescence was measured (B). After phagocytosis, DMEM containing 300 μg/ml of amikacin was added to eliminate extracellular bacteria. Fluorescence (excitation, 485 nm and emission, 520 nm) was measured 1 hour after phagocytosis and plotted as arbitrary units (AU). Error bars correspond to standard errors from four independent experiments. The asterisks indicate *P* values (One way ANOVA, where all strains were compared to WT using Dunnett's multiple comparison post-test, $^{*}P < 0.05$ and $^{***}P < 0.001$), showing statistical significance with respect to WT. (C) PAO1 WT, Δ*mgtC* and Δ*oprF* harboring reporter plasmid pCdrA::*gfp*, were grown in NCE medium with varying concentration of Mg^{2+}. After 1 hour of growth, fluorescence (excitation, 485 nm and emission, 520 nm) of the culture was measured along with its OD_{600nm}. The fluorescence was plotted as arbitrary units (AU_{520nm}) after normalizing with OD_{600nm}. Error bars correspond to standard errors from three independent experiments. The asterisks indicate *P* values showing statistical significance with respect to WT in the respective condition, using Student's t test (ns = $P > 0.05$, $^{*}P < 0.05$, $^{**}P < 0.01$ and $^{***}P < 0.001$).

https://doi.org/10.1371/journal.ppat.1007812.g005

reporter (Fig 5A) that has been validated to gauge c-di-GMP level inside *P. aeruginosa* [38]. The pCdrA::*gfp* plasmid was introduced into wild-type and mutant strains, and fluorescence was measured in infected macrophages (Fig 5B). Both *oprF* and *mgtC* mutants exhibited significantly increased activity of the *cdrA* promoter comparatively to wild-type strain, indicative of higher levels of c-di-GMP than the wild-type strain. To better appreciate the differences monitored within macrophages, we also measured fluorescence of strains grown in culture medium with various magnesium concentrations (Fig 5C). The *oprF* mutant exhibited a two to three-fold increase in the activity of the *cdrA* promoter comparatively to wild-type strain, which is in the same range as the increase observed within macrophages (Fig 5B), and agrees with published data obtained with this indirect strategy and direct c-di-GMP measurement [34]. Under magnesium limitation, a condition known to induce *mgtC* expression, the *mgtC* mutant also showed increased activity of the *cdrA* promoter comparatively to wild-type strain, with a two-fold increase in the absence of Mg^{2+}, and a minor, but significant, increase in the presence of 10 μM Mg^{2+} (that is similar to what is observed within macrophages). On the other hand, the level of fluorescence of wild-type strain and *mgtC* mutant was identical in medium supplemented with 1 mM Mg^{2+}, a condition that prevents *mgtC* expression [25]. Taken together, these results indicate that the production of c-di-GMP is increased relatively to wild-type strain in both *oprF* and *mgtC* mutants, with a more pronounced effect for *oprF*, when bacteria reside within macrophages, thus providing a mechanistic clue for the negative effect on T3SS gene expression.

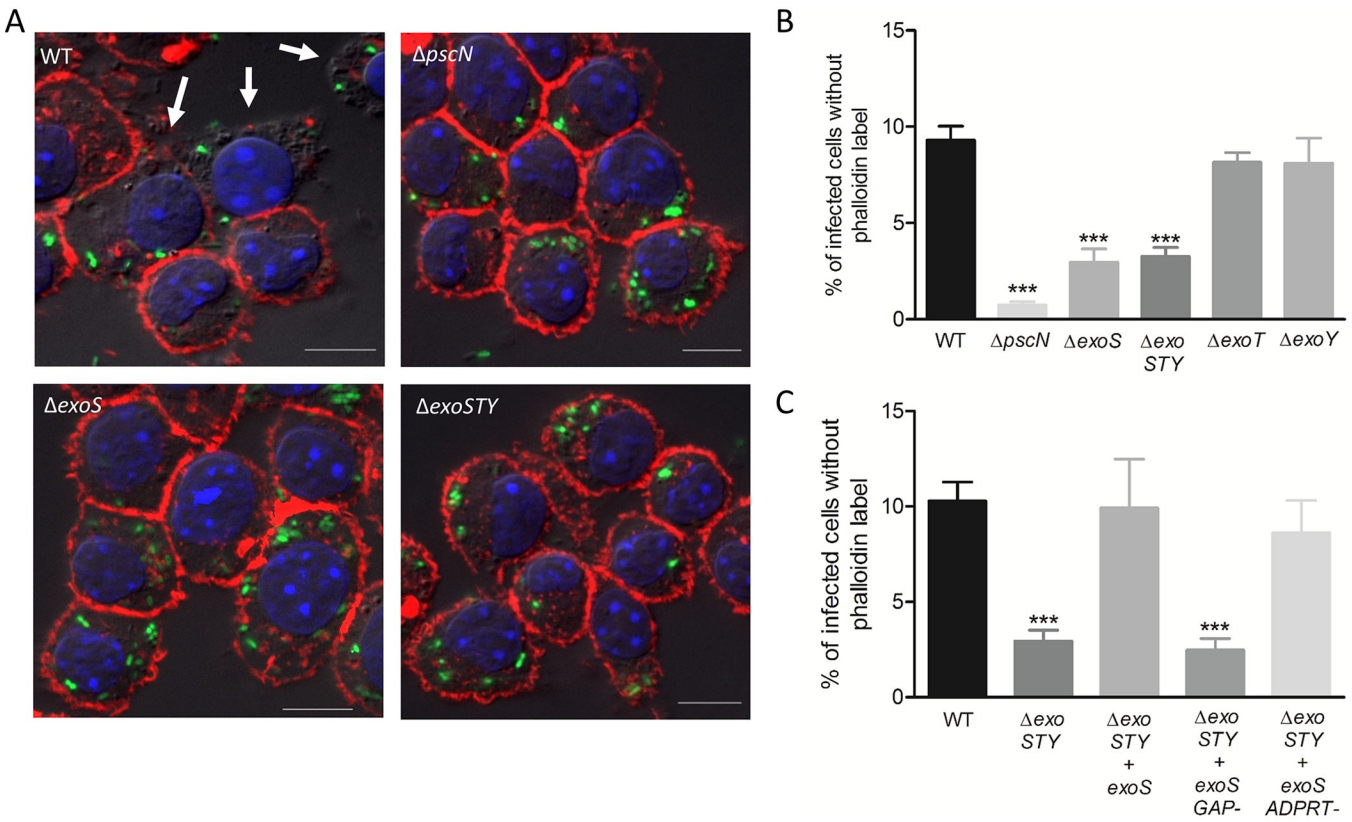

Fig 6. Assessment of role of T3SS and its effectors in cell lysis induced by intracellular PAO1. J774 macrophages were infected with GFP expressing strains as indicated. After phagocytosis, cells were maintained in DMEM supplemented with gentamicin. Cells were imaged 2 hrs post-phagocytosis after staining with phalloidin (A). Scale bar is equivalent to 10 μm. Lysis was quantified (B & C) by counting infected cells lacking cortical labeling (indicated by arrows). Percentage of lysed cells with intracellular bacteria out of total number of infected cells was plotted. Error bars correspond to standard errors from at least three independent experiments. At least 200 cells were counted per strain. The asterisks indicate *P* values (One way ANOVA, where all strains were compared to WT using Dunnett's multiple comparison test, $^{***}P < 0.001$), showing statistical significance with respect to WT.

https://doi.org/10.1371/journal.ppat.1007812.g006

A T3SS mutant is defective for cell death driven intracellularly in an ExoS-dependent manner

Given the effect of both *oprF* and *mgtC* deletions on the expression of T3SS genes within macrophages, we investigated the fate of a T3SS mutant upon phagocytosis. We first used a *pscN* mutant that is defective for the ATPase function of the T3SS machinery [36]. Intracellular T3SS mutant did not induce loss of cortical phalloidin staining, as shown by fluorescent imaging and subsequent quantification, indicating lack of cell lysis (Fig 6A and 6B). Thus, the phenotype of T3SS mutant is consistent with that of *mgtC* and *oprF* mutants and is in correlation with their level of T3SS gene expression. We further examined the relevance of our findings to primary human macrophages, by assessing the lysis of HMDMs driven intracellularly by wild-type *P. aeruginosa* or *oprF* and *pscN* mutants. The count of intracellularly lysed cells was significantly different between wild-type and each mutant strain (Fig 7), with a similar trend to that of J774 macrophages (Fig 3 and Fig 6), thus confirming the importance of T3SS in intracellularly driven lysis of primary human macrophages as well.

To address the implication of T3SS effector proteins in this process, we used mutant strains for individual effector genes *exoS*, *exoT* and *exoY*, and *exoSTY* triple mutant. The intracellular lysis of macrophages was found to be reduced for the *exoSTY* triple mutant and to a similar extent for the *exoS* mutant (Fig 6A and 6B), suggesting a major contribution of ExoS.

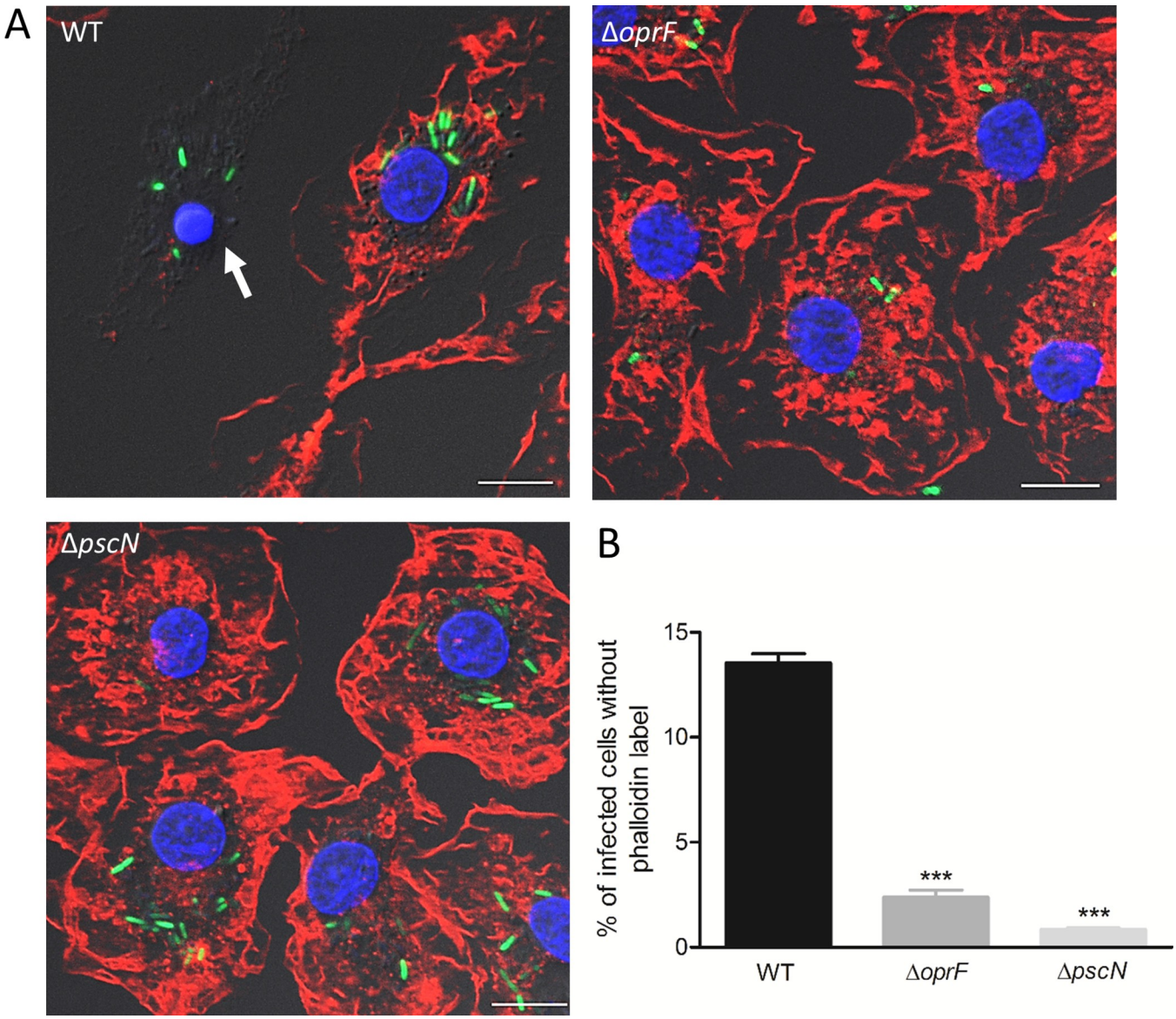

Fig 7. Visualization and quantification of lysis of infected primary human macrophages driven intracellularly by *P. aeruginosa* strains. HMDMs were infected with GFP expressing PAO1 WT, Δ*oprF*, and Δ*pscN* strains. After phagocytosis, cells were maintained in RPMI supplemented with gentamicin. Cells were imaged 2 hrs post-phagocytosis after staining with phalloidin (A) and lysis was quantified (B) by counting infected cells lacking cortical labeling (indicated by arrows). Scale bar is equivalent to 10 μm. Percentage of lysed cells with intracellular bacteria out of total number of infected cells was plotted. Error bars correspond to standard errors from two independent experiments. At least 200 cells were counted per strain. The asterisks indicate *P* values (One way ANOVA, where all strains were compared to WT using Bonferroni's multiple comparison test, $^{***}P < 0.001$), showing statistical significance with respect to WT.

https://doi.org/10.1371/journal.ppat.1007812.g007

Accordingly, *exoT* and *exoY* mutants behave similarly to wild-type strain (Fig 6B). Moreover, complementation of the *exoSTY* mutant with *exoS* restored the wild-type phenotype (Fig 6C). Although the lysis by *exoS* mutant strain was substantially higher than that of *pscN* mutant, these results suggest that the T3SS-mediated intracellular lysis of macrophages by *P. aeruginosa* relies mainly on the T3SS effector ExoS. Thus, this ExoS-dependent cytotoxic effect mediated by intracellular bacteria differs from the classical T3SS-dependent cytotoxicity driven by extracellular bacteria towards macrophages that has been reported to be mostly independent of ExoS [39–41]. To confirm this difference between intracellular and extracellular bacteria

mediated lysis, we measured the lactate dehydrogenase (LDH) release when infection was carried out without removing extracellular bacteria. As expected, similar values were obtained for wild-type strain and *exoS* mutant, whereas a *pscN* mutant showed significantly reduced LDH release (S6 Fig), which agrees with the reported T3SS-dependent but ExoS independent cytotoxicity caused by extracellular bacteria. This is also consistent with trypan blue exclusion assay, which monitors cell death based on penetration of a membrane impermeable dye, when the assay is done immediately after phagocytosis (S7 Fig, panel A).

ExoS possesses GAP domain as well as ADPRT domain and complementing strains retaining only one of these two domains have been constructed earlier [42]. To determine which domain of ExoS plays a role in intracellular cytotoxicity, we carried out the phalloidin-based lysis assay using the *exoSTY* mutant producing either ADPRT (GAP-) or GAP (ADPRT-) domain of ExoS. Our results clearly showed that the strain retaining GAP activity of ExoS but lacking ADPRT activity (Δ*exoSTY* + *exoS* ADPRT-) could complement the phenotype to an extent similar to the strain complemented with *exoS* (Fig 6C), which is also equivalent to the wild-type. To strengthen our findings, we performed trypan blue exclusion assay after 2hrs of gentamicin treatment post-phagocytosis. The results are consistent with phalloidin assay, supporting the implication of ExoS, and more specifically its GAP domain, for macrophage death induced by intracellular bacteria (S7 Fig, panel B). This contrasts with the results of trypan blue exclusion assay performed immediately after phagocytosis, where a low level of T3SS-dependent cell death is observed, but not linked to ExoS function (S7 Fig, panel A).

Hence, our results indicate that, in contrast to extracellular *P. aeruginosa*, intracellular *P. aeruginosa* uses an ExoS-dependent T3SS mediated mechanism to promote macrophage lysis. Moreover, only the GAP activity of ExoS is required for this process.

P. aeruginosa T3SS, *oprF* and *mgtC* mutants displayed lower vacuolar escape than wild-type PAO1

The phagosomal environment of the macrophage is hostile for bacterial pathogens and TEM analysis indicated that PAO1 can be found in the cytoplasm, suggesting escape from the phagosomal vacuole (Fig 2B). We decided to address the intracellular role of T3SS, OprF and MgtC in the phagosomal escape of *P. aeruginosa* to the cytoplasm of macrophages. To monitor *P. aeruginosa* escape from phagosome, we used the CCF4-AM/β-lactamase assay that has been developed for tracking vacuolar rupture by intracellular pathogens [43]. This assay takes advantage of the natural production of β-lactamase by *P. aeruginosa* [44], which can cleave a fluorescent β-lactamase substrate, CCF4-AM, that is trapped within the host cytoplasm. CCF4-AM emits a green fluorescence signal, whereas in the presence of β-lactamase activity, a blue fluorescence signal is produced. The detection of blue fluorescent cells at 2 hrs post-phagocytosis indicated bacterial escape from the phagosome to the cytoplasm (Fig 8A). The escape of wild-type strain was compared to that of *mgtC*, *oprF* and *pscN* mutants by quantifying the percentage of blue fluorescent cells out of total green fluorescent cells. Wild-type strain showed significantly higher percentage of phagosomal escape than all mutants tested (Fig 8B). No significant difference in terms of cleavage of CCF4-AM was measured for the mutants with respect to wild-type in liquid cultures (S8 Fig), indicating that the lower amount of blue fluorescent cells with the mutants is not due to reduced production of endogenous β-lactamase. In agreement with the finding of phagosomal escape by CCF4-AM/β-lactamase assay, ruptured phagosomal membrane could be visualized by TEM in macrophages infected with PAO1 wild-type strain (Fig 8C). Both *exoS* and *exoSTY* effector mutants also displayed a low percentage of phagosomal escape, which appeared similar to that of *pscN* mutant (S9 Fig). These results indicate that the T3SS, through the ExoS effector, plays role in the escape of *P. aeruginosa* from the

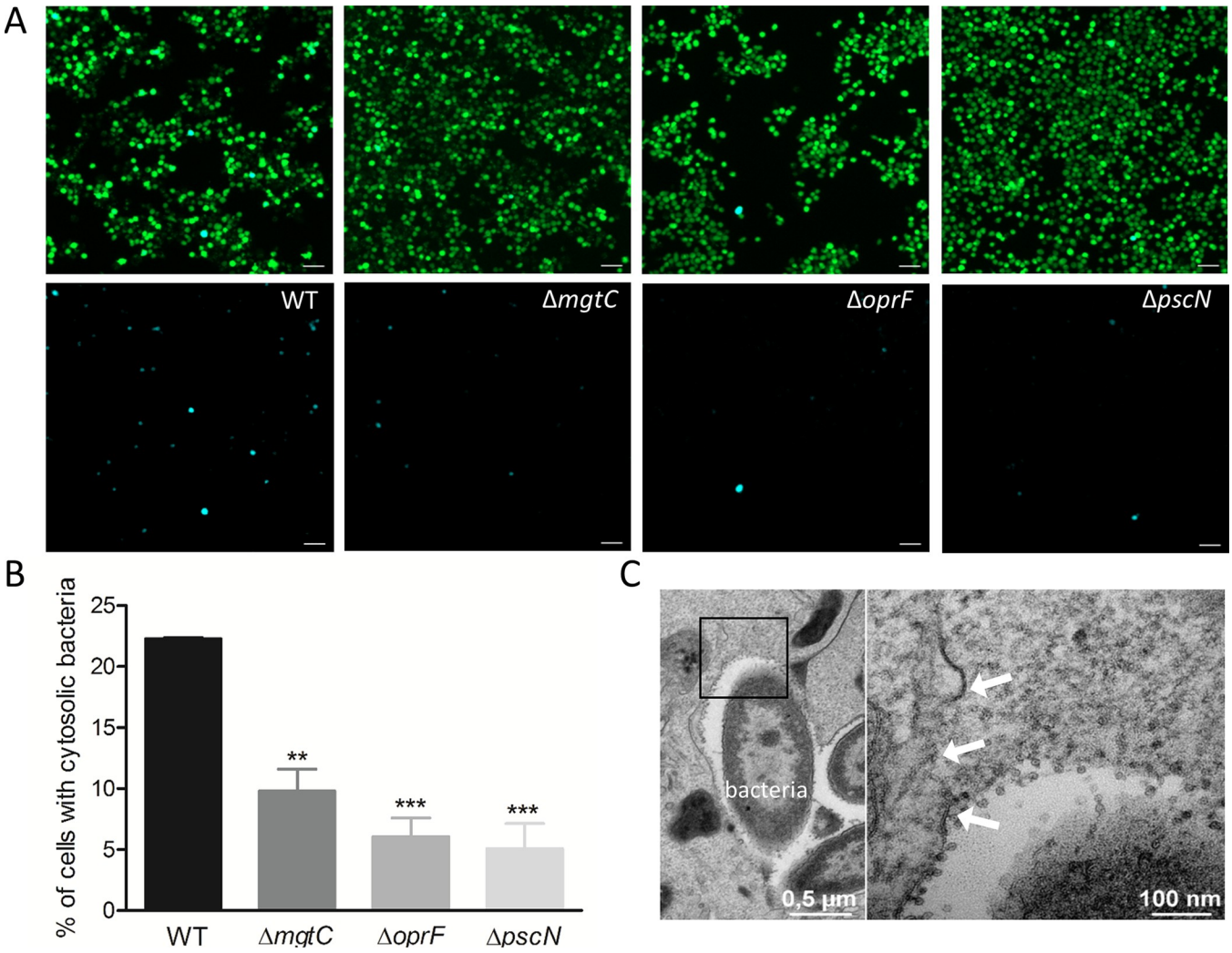

Fig 8. Assessment of access of *P. aeruginosa* to host cytosol using phagosome escape assay. J774 macrophages were infected with PAO1 WT, Δ*mgtC*, Δ*oprF* and Δ*pscN* strains. After phagocytosis, cells were stained with CCF4-AM in presence of gentamicin. 2 hrs post-phagocytosis, the cells were imaged with 10X objective using FITC and DAPI channels. Upon escape of bacteria from phagosome to the cytosol, the CCF4-AM FRET is lost, producing blue color. (A) Representative pictures are shown with the following channels: Total cell population is shown in merged green and blue cells, whereas cells with cleaved CCF4 probe are shown in blue in the lower panel. Scale bar is equivalent to 50 μm. (B) Images were analyzed and quantified by Cell Profiler software to calculate the percentage of blue cells out of total green cells. At least 200 cells were counted per strain. Error bars correspond to standard errors from three independent experiments. The asterisks indicate *P* values (One way ANOVA, where all strains were compared to WT using Dunnett's multiple comparison post-test, $^{**}P < 0.01$ and $^{***}P < 0.001$), showing statistical significance with respect to WT. (C) Electron micrograph showing a disrupted vacuole membrane (white arrows) in a macrophage infected with PAO1 strain. The right panel shows higher magnification of the black square in the left panel.

https://doi.org/10.1371/journal.ppat.1007812.g008

phagosome to the cytoplasm. The effect of MgtC and OprF in this process may as well be mediated by their effect on T3SS gene expression (Fig 4).

Cumulatively, our results support a T3SS-dependent vacuolar escape for *P. aeruginosa*, leading to the localization of bacteria in the cytoplasm and cell lysis as depicted in the proposed model (Fig 9).

Discussion

The ability of professional phagocytes to ingest and kill microorganisms is central to innate immunity and host defense. *P. aeruginosa* is known to avoid being killed by phagocytes through the destruction of immune cells extracellularly as well as avoidance of phagocytosis

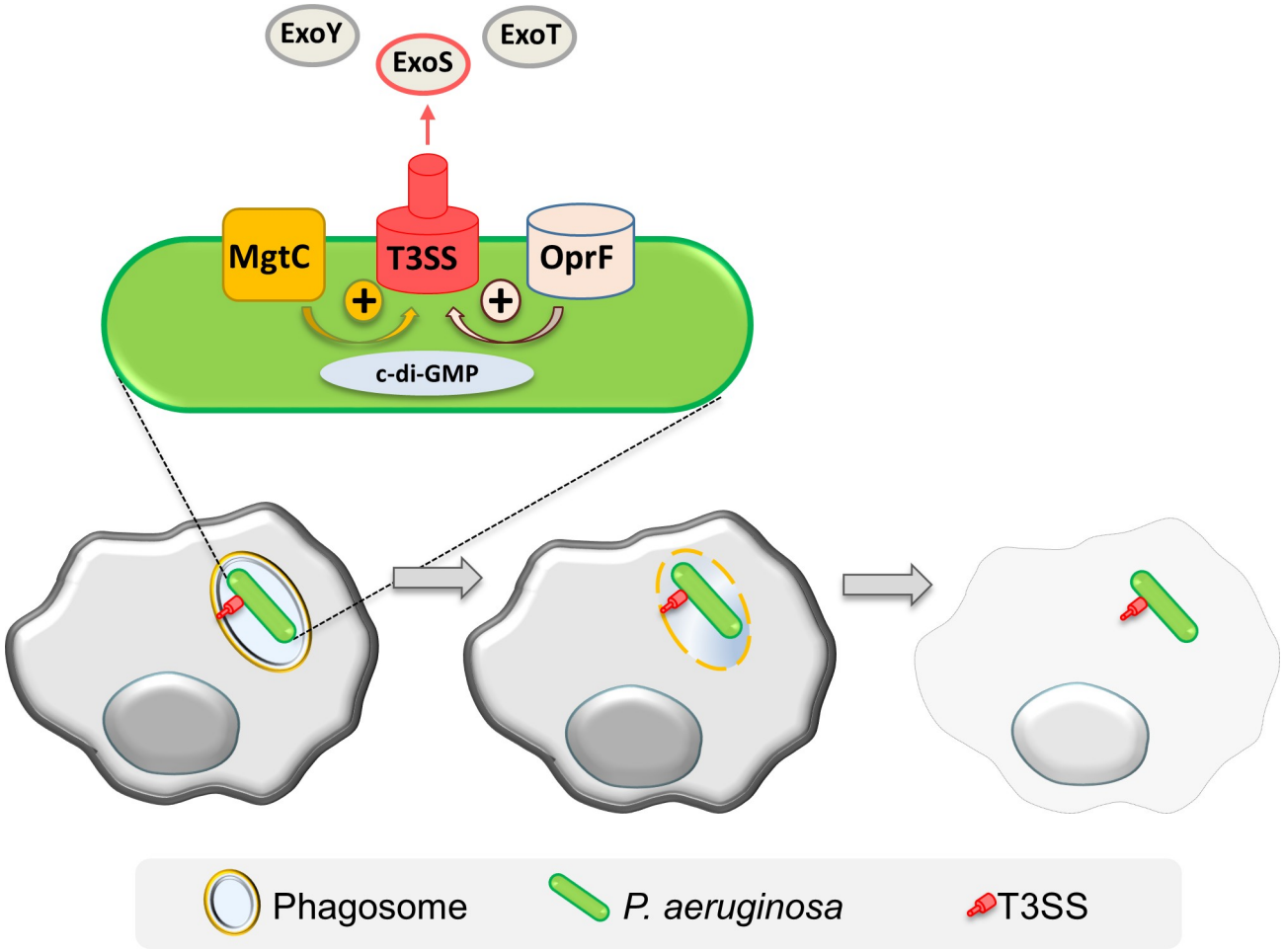

Fig 9. Model for intramacrophage fate of *P. aeruginosa*. Phagocytosed *P. aeruginosa* PAO1 first resides in a vacuole, before escaping the phagosome and promoting macrophage lysis. This cell lysis driven by intracellular *P. aeruginosa* involves the T3SS and more specifically ExoS. MgtC and OprF act positively on the expression of T3SS, possibly by reducing c-di-GMP level, a negative regulator of T3SS expression. Thereby T3SS and its effector ExoS play a role in phagosomal escape and cell lysis. Further work will be required to address secretion of ExoS from intracellularly expressed T3SS as well as identify host targets.

https://doi.org/10.1371/journal.ppat.1007812.g009

[20]. However, *P. aeruginosa* has been reported to be engulfed by macrophages in animal infection models [21–23]. In addition, *P. aeruginosa* has been visualized in phagocytes in cell culture models in several studies, where MgtC and OprF have been shown to be involved in the ability of *P. aeruginosa* to survive in cultured macrophages [25,26]. The virulence of *P. aeruginosa mgtC* mutant can be restored in zebrafish embryos upon macrophages depletion, suggesting that MgtC acts to evade phagocytes [25]. Interestingly, a similar behavior has been reported for a T3SS mutant in the same infection model [21]. We show here that MgtC and OprF regulate T3SS when *P. aeruginosa* resides in macrophages and we describe a novel strategy used by *P. aeruginosa* to escape from macrophages that relies on a T3SS-dependent cell lysis induced by intracellular bacteria (Fig 9).

Using electron microscopy, we demonstrate that upon phagocytosis, *P. aeruginosa* PAO1 strain resides in membrane bound vacuoles, whereas a cytosolic location can be observed at later time of infection, which corroborates the observation of an otopathogenic *P. aeruginosa* clinical strain in HMDMs [26]. Microscopic analysis of live and fixed cells revealed macrophage lysis driven by intracellular bacteria, with J774 macrophage cell line as well as HMDMs. This

cell lysis is a rapid process associated with the loss of cortical actin from plasma membrane. We propose that the cell lysis induced by intracellular *P. aeruginosa* is linked to the phagosomal escape of bacteria as indicated by the observation of cytosolic bacteria and ruptured phagosomal membrane by TEM as well as CCF4-AM/β-lactamase based phagosomal rupture assay.

To better characterize the *P. aeruginosa* factors involved in its intramacrophage fate, we investigated intracellular expression of T3SS genes in *mgtC* and *oprF* mutants. Expression of T3SS genes upon macrophage infection was significantly decreased in *mgtC* mutant and abrogated in *oprF* mutant. The production of T3SS effectors or needle component was previously known to be altered in the *oprF* mutant [32,34], but a direct effect at the transcriptional level was not investigated before. This regulation could be mediated by c-di-GMP, a known negative regulator of T3SS expression [37], as the reporter assay revealed an increased level of c-di-GMP in both *oprF* and *mgtC* mutants upon monitoring infected macrophages, with a more pronounced effect for *oprF* mutant. An increased level of c-di-GMP in *oprF* mutant is consistent with previous results obtained *in vitro* [34]. The moderate, but significant, increase in the level of c-di-GMP in *mgtC* mutant in macrophages with respect to wild-type strain is equivalent to the fold increase obtained in low-Mg^{2+} cultures. It is of interest to note that a *Salmonella mgtC* mutant also exhibited increased c-di-GMP level intracellularly and under low-Mg^{2+} condition [29]. The *P. aeruginosa mgtC* and *oprF* mutants showed a moderate and a more pronounced decrease, respectively, in cytotoxicity driven by intracellular bacteria and phagosomal escape. These phenotypes could be linked to the pattern of T3SS expression in *mgtC* and *oprF* mutants because a T3SS mutant appeared to lack cytotoxicity driven by intracellular bacteria and showed reduced phagosomal escape. Accordingly, inducing expression of *exsA* gene, a master activator of T3SS, in *oprF* mutant promoted macrophage lysis driven by intracellular bacteria to a similar level to that of wild-type strain, supporting the model whereby the phenotype of *oprF* mutant is the result of a negative regulation of T3SS expression.

Our data indicate that the T3SS-mediated cytotoxicity driven by intracellular *P. aeruginosa* is largely dependent on the ExoS effector. ExoS, which has a dual function [10], was known to play a role in the intracellular life of *P. aeruginosa* in cell types other than macrophages. The T3SS and ExoS are indeed key factors for intracellular replication of *P. aeruginosa* in epithelial cells, with a main role of the ADPRT domain in the formation of replicative niche in membrane blebs [18,19,45]. ExoS and ExoT ADPRT domains also promote bacterial survival in neutrophils [46], by having a protective role against NADPH-oxidase activity [47]. However, the effect of T3SS towards macrophages was so far restricted to the well-known cytotoxicity caused by extracellular *P. aeruginosa* [39,48–50]. In *P. aeruginosa* strains lacking ExoU toxin, such as PAO1, this cytotoxicity is due to inflammasome activation, which is dependent on T3SS translocation apparatus, but is independent of the ExoS effector [39–41,51]. Accordingly, this T3SS-dependent ExoS-independent cytotoxity was observed in our assays when extracellular bacteria were not removed. In contrast, upon removal of extracellular bacteria, a T3SS-mediated cytotoxicity implicating ExoS was uncovered. Hence, ExoS appears to be associated with cell damage only when it is secreted from internalized bacteria. Moreover, phagosomal rupture assay indicated that ExoS plays role in the escape of *P. aeruginosa* from the phagosome to the cytoplasm and we propose that upon phagosomal rupture, the cytoplasmic location of *P. aeruginosa* induces inflammasome, possibly through the release of bacterial lipopolysaccharides (LPS) in the cytoplasm, which would promote cell death. Therefore, in addition to the inflammasome activation caused by extracellular *P. aeruginosa* and, as very recently described, by intracellular T3SS-negative *P. aeruginosa* in the context of long-term infection [52], our study suggests that inflammasome and subsequent macrophage death can also be caused by intracellular T3SS-positive *P. aeruginosa*. Further studies will be required to characterize inflammasome activation and pathways that lead to cell death.

The intracellular implication of ExoS in both macrophages and epithelial cells suggests that the intracellular life of *P. aeruginosa* in macrophages shares features with the intracellular life of the pathogen in epithelial cells, even though the outcome is different. While bacteria actively replicate in epithelial cells, within bleb niches or in the cytosol [17], replication of bacteria is barely seen within macrophages resulting instead in cell lysis and bacterial escape from macrophages. Our results further indicate that the macrophage damage caused by intracellular *P. aeruginosa* is due to ExoS GAP domain, which thus differs from the reported role of the ADPRT domain of ExoS in blebs formation associated with intracellular replication of *P. aeruginosa* within epithelial cells [18,19,45]. On the other hand, the implication of GAP domain of ExoS towards epithelial cells in promoting cell rounding, actin reorganization or cell death has not been specifically associated with intracellular bacteria [53,54]. Although ExoS and ExoT GAP domain have similar biochemical activities, these effectors may differ in their localization inside host cells or they may interact with different host factors to bring about their effect. This is supported by the fact that apoptosis is induced in epithelial cells by ExoT GAP domain, a feature that was not reported for ExoS GAP domain [55] and by our finding that, unlike ExoS, ExoT is not involved in the intramacrophage phenotypes. Importantly, we show that the extent of phagosomal escape of *pscN* and *exoSTY* mutants was similar to that of *exoS* mutant alone, suggesting that ExoS is the main effector protein involved in the exit of *P. aeruginosa* from the phagosome. In epithelial cells, ExoS has been involved in avoidance of acidified compartment [18,19]. Considering our findings, ExoS may allow avoidance of acidification in macrophages and may also contribute to the vacuolar escape in epithelial cells. Further studies will be required to decipher in more detail, the function of ExoS inside macrophages, including a better understanding of its role in phagosomal escape and identification of its host targets within macrophages. ExoS-positive strains represent a large number of clinical isolates but the number of ExoS-negative strains is nevertheless substantial (about one third of isolates), especially among strains associated with bacteremia [10,11,56]. However, strains lacking ExoS usually encode the potent cytotoxin ExoU, thus exhibiting high toxicity towards eukaryotic cells from outside and less susceptibility to encounter an intracellular stage.

In conclusion, our results indicate that *P. aeruginosa* shares common feature with other so-called extracellular pathogens, such as *S. aureus*, which can reside transiently within macrophages [4] and require bacterial factors to survive this stage [57]. The present study uncovered bacterial factors allowing internalized *P. aeruginosa* to lyse macrophages. This should let bacteria to evade macrophages and an important issue now is to better evaluate the contribution of intramacrophage stage to disease outcome during *P. aeruginosa* infection. Survival of *P. aeruginosa* within macrophages and subsequent bacterial release may play a role in the establishment and dissemination of infection. There is also evidence that intracellular survival may contribute to persistence of the infection by creating a niche refractory to antibiotic action [24], highlighting the potential importance of this overlooked phase of *P. aeruginosa* infection.

Materials and methods

Bacterial strains and growth conditions

Bacterial strains and plasmids are described in Table 1. *P. aeruginosa* mutant strains (all in the PAO1 background) have been described and phenotypically characterized previously (Table 1). The *oprF* mutant (strain H636) is derived from PAO1 wild-type strain H103 [34], which exhibits the same level of ExoS secretion under T3SS-inducing conditions as PAO1, the isogenic strain for *mgtC* and T3SS mutants (S10 Fig). *P. aeruginosa* was grown at 37˚C in Luria broth (LB). Growth in magnesium-defined medium was done in NCE-minimal medium [58] supplemented with 0.1% casamino acids, 38 mM glycerol, without $MgSO_4$ or containing

Table 1. Bacterial strains and plasmids used in the study.

Name	Description	Reference
PAO1		Laboratory collection
PAO1 Δ*mgtC*	Δ*mgtC*	[25]
H636	Δ*oprF*	[34]
PAO1 Δ*pscN*	Δ*pscN* T3SS ATPase mutant	[36]
PAO1 Δ*exoS*	Δ*exoS*	[50]
PAO1 Δ*exoY*	Δ*exoY*	[50]
PAO1 Δ*exoT*	Δ*exoT*	[50]
PAO1 Δ*exoSTY*	Δ*exoSTY*	[50]
PAO1FΔ3Tox/ExoS	Δ*exoS* Δ*exoT* Δ*exoY attB*::*exoS*	[42]
PAO1FΔ3Tox/ExoS$_{GAP}$-	Δ*exoS* Δ*exoT* Δ*exoY attB*::*exoS*-$R_{146}K$	[42]
PAO1FΔ3Tox/ExoS $_{ADPR}$ -	Δ*exoS* Δ*exoT* Δ*exoY attB*::*exoS*-$E_{379}D/E_{381}D$	[42]
pRK2013	Tra$^+$, Mob$^+$, ColE1, Km^r	Laboratory collection
pMF230	GFP*mut2*, Amp^r	[59]
pTn7CdrA::*gfp*^{C}	Amp^r, Gm^r	[38]
pSBC6	*exsA* cloned in pMMB190 under control of *tacp* Amp^r	[36]

https://doi.org/10.1371/journal.ppat.1007812.t001

10 μM or 1mM $MgSO_4$. Plasmid pMF230 expressing GFP constitutively [59] (obtained from Addgene), was introduced in *P. aeruginosa* by conjugation, using an *E. coli* strain containing helper plasmid pRK2013. Recombinant bacteria were selected on *Pseudomonas* isolation agar (PIA) containing carbenicillin at the concentration of 300 μg/ml.

Infection of J774 macrophages

J774 cells (murine macrophage cell line J774A.1, gifted by Gisèle Bourg, Inserm U 1047, Nîmes, France) were maintained at 37˚C in 5% CO_2 in Dulbecco's modified Eagle medium (DMEM) (Gibco) supplemented with 10% fetal bovine serum (FBS) (Gibco). The infection of J774 macrophages by *P. aeruginosa* was carried out essentially as described previously [25]. Mid-log phase *P. aeruginosa* grown in LB broth was centrifuged and resuspended in PBS to infect J774 macrophages (5×10^5 cells/well) at an MOI of 10. After centrifugation of the 24-well culture plate for 5 min for synchronization of infection, bacterial phagocytosis was allowed for 25 min. Cells were washed three times with sterile PBS and fresh DMEM medium supplemented with 400 μg/ml gentamicin was added and retained throughout the infection.

Infection of human primary macrophages

Purified monocytes isolated as described from blood of healthy donors were frozen in liquid nitrogen [60,61]. Cells were thawed for experiment and seeded onto 24-well plates at a density of $7x10^5$ per well in complete culture medium (RPMI containing 10% FCS) and differentiated into macrophages with rh-M-CSF (10 ng/ml) (purchased from Al-Immuno tools) for 7 days. HMDMs were infected with exponentially growing *P. aeruginosa* cultures (OD_{600} = 0.8) at an MOI of 10, as described above.

Live microscopy

J774 macrophages were seeded in ibidi μ-slide (8 wells) in DMEM medium supplemented with 10% FBS and infected with *P. aeruginosa* PAO1 expressing GFP as described in the

previous section. Imaging started after 30 min of phagocytosis, when the media was changed to DMEM supplemented with 400 μg/ml gentamicin until 3 hrs post phagocytosis. Cells were imaged using an inverted epifluorescence microscope (AxioObserver, Zeiss), equipped with an incubation chamber set-up at 37˚C and 5% CO_2 and a CoolSNAP HQ2 CCD camera (Photometrics). Time-lapse experiments were performed, by automatic acquisition of random fields using a 63X Apochromat objective (NA 1.4). The frequency of acquisition is indicated in figure legends. Image treatment and analysis were performed using Zen software (Zeiss).

Transmission electron microscopy

Macrophages were seeded on glass coverslips and infected as described above. Infected cells were fixed for 4 hrs at room temperature with 2.5% gluteraldehyde in cacodylate buffer 0.1 M pH 7.4 with 5mM $CaCl_2$, washed with cacodylate buffer, post-fixed for 1 hr in 1% osmium tetroxide and 1.5% potassium ferricyanide in cacodylate buffer, washed with distilled water, followed by overnight incubation in 2% uranyl acetate, prepared in water. Dehydration was performed through acetonitrile series and samples were impregnated in epon 118: acetonitrile 50:50, followed by two times for 1 hr in 100% epon. After overnight polymerization at 60˚C, coverslips were detached by thermal shock with liquid nitrogen. Polymerization was then prolonged for 48 hrs at 60˚C. Ultrathin sections of 70 nm were cut with a Leica UC7 ultramicrotome (Leica microsystems), counterstained with lead citrate and observed in a Jeol 1200 EXII transmission electron microscope. All chemicals were from Electron Microscopy Sciences (USA) and solvents were from Sigma. Images were processed using Fiji software.

Colocalization of *P. aeruginosa* with acidic compartments

Macrophages were infected with GFP labelled *P. aeruginosa* as described above. After 2.5 hrs of gentamicin treatment, infected J774 cells were washed twice with PBS and incubated with 50 nM Lysotracker red DND-99 (Molecular Probes) in DMEM for 10 min to stain lysosomes. Cells were then washed with PBS and fixed with 4% paraformaldehyde in PBS and mounted on glass slides in Vectashield (Vector Laboratories, Inc) with 4′,6-diamidino-2-phenylindole (DAPI) to stain the nucleus. The slides were examined using an upright fluorescence microscope (Axioimager Z2, Zeiss) equipped with an Apotome 1 for optical sectioning. A 63X Apochromat Objective (NA 1.4) was used, transmitted light was acquired using differential interference contrast (DIC), Fluorescein isothiocyanate (FITC) filter was used to visualize GFP expressing bacteria and Lysotracker red fluorescence was acquired using a texas red filter set.

Phalloidin labeling

J774 macrophages were seeded on glass coverslips and infected with GFP expressing bacteria as described in the previous sections. For cytochalasin treatment, DMEM containing 2 μM cytochalasin D (Sigma) was added to the macrophages 1 hour before infection and maintained during phagocytosis. After phagocytosis, the cells were maintained in 1 μM cytochalasin D till the end of the experiment. For untreated control, 0.2% DMSO (solvent control) in DMEM was added to the cells before and during phagocytosis. After phagocytosis, cells were maintained in 0.1% DMSO. After fixation with 4% paraformaldehyde (EMS, USA) in PBS for 5 min, cells were washed once with PBS and permeabilized by adding 0.1% triton X-100 for 1 min 30 sec. Cells were then washed once with PBS and incubated with 1 μg/ml Tetramethylrhodamine B isothiocyanate (TRITC)-labeled phalloidin (Sigma-Aldrich) in PBS for 30 min in dark. Cells were washed twice with PBS and coverslips were mounted on glass slides in Vectashield with DAPI (Vector Laboratories, Inc). The slides were examined using an upright

fluorescence microscope (Axioimager Z1, Zeiss) equipped with an Apotome 1 for optical sectioning. A 63X Apochromat Objective (NA 1.4) was used and transmitted light was acquired using DIC. FITC and texas red filters were used to visualize GFP expressing bacteria and phalloidin respectively. Cell nuclei were visulalized using DAPI filter. Images were processed using ZEN software (Zeiss). Cells were counted manually, where infected cells lacking the phalloidin stain were considered as lysed. Percentage of such lysed cells with intracellular bacteria out of total number of infected cells was calculated and plotted for each strain.

Strains containing pSBC6 plasmid (expressing *exsA* under the control of *tac* promoter) were grown before infection in LB or in LB supplemented with 0.01 mM IPTG. Because these strains did not harbor GFP producing plasmid, the number of total cells without phalloidin label was counted and percentage out of total number of cells was plotted. The percent of lysed cells for wild-type strain was similar to that found with GFP positive PAO1 strain.

LDH cytotoxicity assay

The cytotoxicity was assessed by release of LDH from infected J774 macrophages infected, using the Pierce LDH cytotoxicity assay kit (Thermo Scientific). Macrophages were infected for 2 hrs at an MOI of 10 as described above, except that cells were seeded in a 96 well plate and extracellular bacteria were not removed. The assay was performed on 50 μl of the culture supernatant according to manufacturer's instructions. LDH release was obtained by subtracting the 680 nm absorbance value from 490 nm absorbance. The percentage of LDH release was first normalized to that of the uninfected control and then calculated relatively to that of uninfected cells lysed with Triton X-100, which was set at 100% LDH release.

Trypan Blue exclusion test of cell viability

The membrane impermeable dye Trypan Blue was used to quantify cell viability after phagocytosis or after 2 hrs of gentamicin treatment following phagocytosis. Trypan Blue stain (0.4%) was added in 1:1 ratio with PBS for 3 min at room temperature, replaced by PBS and the cells were imaged using an optical microscope in bright field mode. Dead cells appear blue as they take up the stain, in contrast to healthy cells that appear transparent because of the exclusion of the dye. Cells were counted and the percentage of dead cells out of total cells (blue + colorless) was calculated.

RNA extraction and quantitative RT-PCR (qRT-PCR)

For bacterial RNA extraction from infected J774, $6.5x10^6$ macrophages were seeded into a 100 cm^2 tissue culture dish and infected at an MOI of 10 as described above. 1 hour after phagocytosis, cells were washed three times with PBS, lysed with 0.1% Triton X100 and pelleted by centrifugation at 13000 rpm for 10 min at 15˚C. Bacteria were resuspended in 500 μl PBS and the non resuspended cellular debris was discarded. 900 μl of RNA protect reagent (Qiagen) was added and incubated for 5 min. The sample was centrifuged at 13000 rpm for 10 min. Bacteria in the pellet were lysed with lysozyme and RNA was prepared with RNeasy kit (Qiagen). Superscript III reverse transcriptase (Invitrogen) was used for reverse transcription. Controls without reverse transcriptase were done on each RNA sample to rule out possible DNA contamination. Quantitative real-time PCR (q-RT-PCR) was performed using a Light Cycler 480 SYBR Green I Master mix in a 480 Light Cycler instrument (Roche). PCR conditions were as follows: 3 min denaturation at 98˚C, 45 cycles of 98˚C for 5 sec, 60˚C for 10 sec and 72˚C for 10 sec. The sequences of primers used for RT-PCR are listed in S1 Table.

Cyclic di-GMP reporter assay

The strains were transformed by electroporation with the plasmid pCdrA::*gfp* [34,38], which expresses GFP under the control of the promoter of *cdrA*, a c-di-GMP responsive gene, and carries a gentamicin resistance gene. Overnight cultures, grown in LB with 100 μg/ml gentamicin, were subcultured in LB. These cultures were used to infect J774 cells seeded in a 96 well plate (Greiner, Flat-Bottom), containing 10^5 cells per well with an MOI of 20 after normalizing the inoculum to their OD_{600}. After phagocytosis, DMEM containing 300 μg/ml of amikacin, instead of gentamicin, was added to eliminate extracellular bacteria, as these strains are resistant to gentamicin. At the required time point, Tecan fluorimeter (Spark 20M) was used to measure fluorescence (excitation, 485 nm and emission, 520 nm) of cells at the Z point where emission peak could be obtained in comparison to the blank. Fluorescence was plotted for each strain in terms of arbitrary units (AU). CdrA activity of all strains was also measured in liquid cultures under changing concentrations of magnesium. All strains, grown overnight in LB, were diluted in LB and grown until OD_{600} of 0.6, washed in NCE medium without magnesium and resuspended in NCE medium containing 1 mM, 10 μM or no magnesium for 1 hour in 96 well plate (Greiner, Flat-Bottom). Their fluorescence (excitation, 485 nm and emission, 520 nm) and OD_{600nm} were measured. Fluorescence (AU_{520nm}) was normalized to OD_{600nm} and plotted for each strain.

CCF4 fluorometric assay to monitor the escape of *P. aeruginosa* in host cytosol

The vacuole escape assay was adapted from the CCF4 FRET assay [43] using the CCF4-AM LiveBlazer Loading Kit (Invitrogen) and an image-based quantification [62]. Briefly, J774 macrophages were seeded in 96 well plate (Greiner, Flat-Bottom), containing $5x10^4$ cells per well. Overnight bacterial cultures were subcultured in LB with 50 μg/ml of ampicillin to enhance the expression of beta-lactamase, present naturally in *P. aeruginosa*. Infection was carried out as mentioned in the previous sections at the MOI of 10. After phagocytosis, the cells were washed thrice with PBS to remove extracellular bacteria. 100 μl of HBSS buffer containing 3 mM probenecid and gentamicin (400 μg/ml), was added in each well. The substrate solution was prepared by mixing 6 μl of CCF4-AM (solution A), 60 μl of solution B and 934 μl of solution C. 20 μl of the substrate solution was added to each well and the plate was incubated in dark at 37˚C with 5% CO_2. After 2 hrs, the cells were imaged as described in the Live Imaging section, using a 10X objective. FITC and DAPI channels were used to visualize CCF4-FRET (Green) and loss of FRET (Blue) respectively. Each sample was taken in triplicate and image acquisition was performed by automated random acquisition. Images were analyzed by Cell Profiler software to calculate the number of blue and green cells. The threshold for detection of blue signal by the software was normalized to uninfected control i.e. no blue cells could be detected in the uninfected control. The percentage of blue cells, representing the cells with cytosolic bacteria, out of total green cells was plotted. All strains were tested for their ability to cleave CCF4 *in vitro*, before carrying out the vacuole rupture assay. Overnight cultures grown in LB were subcultured at the ratio of 1:20 in LB with 100 μg/ml of ampicillin. After 2 hours of growth, the cultures were centrifuged and resuspended in PBS. 100 μl of this was aliquoted in 96 well plate (Greiner, Flat-Bottom) and 20 μl of CCF4 substrate solution (A+B +C) was added. Tecan fluorimeter (Spark 20M) was used to measure fluorescence (excitation, 405 nm and emission, 450 nm) using PBS as blank. Blue fluorescence (AU_{450nm}) was observed for all strains and none of the mutants exhibited significantly lower value than the wild-type strain.

Ethics statement

Monocytes were issued from blood of anonymous donors obtained from the French blood bank (Etablissement Français du Sang, approval EFS-OCPM n˚ 21PLER2018-0057).

Supporting information

S1 Fig. Live imaging of macrophages infected with *P. aeruginosa*. J774 macrophages were infected with PAO1 wild-type strain expressing GFP. Time lapse imaging was started at 1.5 hrs post-phagocytosis. Cells were maintained in DMEM supplemented with gentamicin, at 37˚C and 5% CO_2 throughout imaging. White arrows point at infected cells that undergo lysis, whereas black arrows indicate uninfected cells that do not lyse. Images were taken between 1.5 hrs and 3 hrs post-phagocytosis as shown on the panels. Scale bar is equivalent to 10 μm.
(PDF)

S2 Fig. Live imaging of primary human macrophages infected with *P. aeruginosa*. HMDMs were infected with PAO1 wild-type (WT) strain expressing GFP. Time lapse imaging was started at 1.5 hrs post-phagocytosis. Cells were maintained in RPMI supplemented with gentamicin at 37˚C and 5% CO_2 throughout imaging. White arrows point at the cells that harbor intracellular bacteria and undergo lysis between 1.5 hrs and 3 hrs post-phagocytosis. Black arrow shows an uninfected and unlysed cell. Scale bar is equivalent to 20 μm.
(PDF)

S3 Fig. Colocalization of *P. aeruginosa* with a probe that labels acidic compartments. J774 macrophages were infected with PAO1 expressing GFP. After 2.5 hrs of gentamicin treatment, infected J774 cells were incubated with Lysotracker for 10 min, a red fluorescent weak base that accumulates in acidic compartments. Cells were then fixed and imaged with fluorescence microscope. (A) The image shows individual panels for Differential Interference Contrast (DIC), lysosomal compartment (red), bacteria expressing GFP (green), the nucleus (blue) and merged image of all channels. The solid arrow shows colocalization of bacteria with lysotracker and dashed arrow shows non-colocalization. Scale bar is equivalent to 5 μm. (B) 3D-reconstructed image of the same area of (A).
(PDF)

S4 Fig. Visualization (A) and quantification (B) of lysed infected cells upon cytochalasin D treatment. GFP expressing PAO1 was used for infecting J774 macrophages. DMEM containing 2 μM cytochalasin D was added to the macrophages 1 hour before infection and maintained during phagocytosis. After phagocytosis, cells were maintained in 1 μM cytochalasin D in DMEM supplemented with gentamicin till the end of the experiment. 0.2% DMSO in DMEM was added to the cells as solvent control before and during phagocytosis. After phagocytosis, cells were maintained in 0.1% DMSO in DMEM with gentamicin, fixed 2 hrs post-phagocytosis, stained with phalloidin and imaged with fluorescent microscope. DAPI was used to stain the nucleus. Cells that have intracellular bacteria, but lack the phalloidin cortical label, were considered as lysed by intracellular bacteria (shown by arrows). Scale bar is equivalent to 10 μm. Percentage of lysed cells with intracellular bacteria out of total number of cells was plotted. Error bars correspond to standard errors from two independent experiments. At least 200 cells were counted per strain. The asterisks indicate *P* values (Student's t-test, $^{**}P < 0.01$), showing statistical significance with respect to DMSO control.
(PDF)

S5 Fig. Quantification of dying cells infected with *P. aeruginosa* strains overexpressing *exsA*. PAO1 WT, Δ*oprF*, PAO1 WT + p*exsA* and Δ*oprF* + p*exsA* strains were used for infecting J774 macrophages. Expression of *exsA* was induced by adding 0.01 mM IPTG for the strains PAO1 WT + p*exsA* and Δ*oprF* + p*exsA*. Gentamicin was added after phagocytosis and cells were fixed at 2 hrs post-phagocytosis, stained with phalloidin and imaged with fluorescent microscope. DAPI was used to stain the nucleus. Cells that lacked the phalloidin cortical label

were considered as lysed by intracellular bacteria. After imaging, percentage of lysed cells out of total number of cells was plotted for each strain. Error bars correspond to standard errors from at least three independent experiments. At least 200 cells were counted per strain. The asterisks indicate *P* values (One way ANOVA, where all strains were compared to each other using Bonferroni's multiple comparison post-test, $^{**}P < 0.01$ and ns = $P > 0.05$), showing statistical significance with respect to WT.
(PDF)

S6 Fig. Quantification of cell lysis driven by extracellular bacteria. Release of LDH was measured from J774 macrophages infected for 2 hrs with PAO1 WT, Δ*pscN*, Δ*exoS* and Δ*exoSTY* strains to quantify the cytotoxicity. The percentage of LDH release was calculated relatively to that of total uninfected cells lysed with Triton X-100, which was set at 100% LDH release. Error bars correspond to standard errors (SE) from at least four independent experiments. The asterisks indicate *P* values (One way ANOVA, where all strains were compared to WT using Dunnett's multiple comparison post-test, $^{**}P < 0.01$), showing statistical significance with respect to WT.
(PDF)

S7 Fig. Quantification of lysed cells by staining with Trypan Blue. J774 macrophages were infected with the strains as indicated. After phagocytosis, cells were maintained in DMEM supplemented with gentamicin. Cells were stained with trypan blue at (A) 30 min or (B) 2 hrs post-phagocytosis and imaged. Lysed cells were quantified by counting cells stained with trypan blue and the percentage of lysed cells out of total number of cells was plotted. Error bars correspond to standard errors from at least three independent experiments. At least 400 cells were counted per strain. The asterisks indicate *P* values (One way ANOVA, where all strains were compared to WT using Dunnett's multiple comparison test, $^{*}P < 0.05$, $^{**}P < 0.01$ and $^{***}P < 0.001$), showing statistical significance with respect to WT.
(PDF)

S8 Fig. Assessment of β-lactamase activity in liquid culture. PAO1 WT, Δ*mgtC*, Δ*oprF*, Δ*pscN*, Δ*exoS* and Δ*exoSTY* strains grown in presence of ampicillin, were incubated with CCF4-AM for 1 hour. The blue fluorescence generated as a result of loss of FRET of CCF4 was measured (excitation, 420 nm and emission, 450 nm) and plotted as arbitrary units (AU). Error bars correspond to standard errors from four independent experiments. All strains were compared to WT using One way ANOVA, Dunnett's multiple comparison post-test. No significant difference was found between the mutant strains and WT.
(PDF)

S9 Fig. Phagosome escape assay of T3SS mutants. J774 macrophages were infected with PAO1 WT, Δ*pscN*, Δ*exoS* and Δ*exoSTY* strains. After phagocytosis, cells were stained with CCF4-AM in presence of gentamicin. 2 hrs post-phagocytosis, the cells were imaged with 10X objective using FITC and DAPI channels. Upon escape of bacteria from phagosome to the cytosol, the CCF4-AM FRET is lost, producing blue color. Images were analyzed and quantified by Cell Profiler software to calculate the percentage of blue cells out of total green cells. At least 200 cells were counted per strain. Error bars correspond to standard errors from four independent experiments. The asterisks indicate *P* values (One way ANOVA, where all strains were compared to WT using Dunnett's multiple comparison post-test, $^{*}P < 0.05$), showing statistical significance with respect to WT.
(PDF)

S10 Fig. Comparison of secreted protein profiles and ExoS production under T3SS-inducing conditions in two PAO1 strains. Immunodetection of the ExoS effector in culture

supernatant of PAO1 and PAO1 H103 (isogenic WT strain for *oprF* mutant) grown in exponential phase at 37˚C under T3SS-inducing (– Ca^{2+}) or non-inducing (+ Ca^{2+}) conditions. The bacterial culture supernatant (equivalent of 1 OD_{600} unit) was loaded on an SDS gel containing 10% polyacrylamide. As control, cellular fraction (equivalent of 0.1 OD_{600} unit) was loaded. Upper panels show Western blot using anti-ExoS antibodies (Soscia et al., 2007; doi: 10.1128/JB.01677-06) and lower panels show Coomassie stained gels.
(PDF)

S1 Movie. Live microscopy movie imaging cell lysis in real time. J774 macrophages were infected with PAO1 WT strain expressing GFP. Cells were maintained in DMEM supplemented with gentamicin, at 37˚C and 5% CO_2 throughout imaging. Imaging was started at 3 hrs post-phagocytosis and continued for 10 min with interval of 30 sec between frames. The time frame is displayed in the movie in the format of minutes:seconds:milli seconds. The movie shows quick lysis of macrophages harboring intracellular bacteria occurring within a minute.
(MOV)

S1 Table. List of primers used for RT-PCR.
(PDF)

Acknowledgments

We thank Sylvie Chevalier (Rouen), Ina Attrée and Sylvie Elsen (Grenoble) for providing strains and plasmids, the Montpellier RIO Imaging microscopy platform for photonic Microscopy and the Electron Microscopy facility of the University of Montpellier (MEA) for sample preparation and transmission electron microscopy. We thank Bérengère Ize and Laila Gannoun-Zaki for critical reading of the manuscript, Matteo Bonazzi and Fernande Siadous for their expertise with the CCF4 assay, Chantal Soscia for testing ExoS secretion.

Author Contributions

Conceptualization: Preeti Garai, Laurence Berry, Anne-Béatrice Blanc-Potard.

Data curation: Preeti Garai.

Formal analysis: Preeti Garai, Malika Moussouni.

Funding acquisition: Anne-Béatrice Blanc-Potard.

Investigation: Preeti Garai, Laurence Berry, Malika Moussouni, Anne-Béatrice Blanc-Potard.

Methodology: Preeti Garai, Laurence Berry, Anne-Béatrice Blanc-Potard.

Project administration: Anne-Béatrice Blanc-Potard.

Resources: Sophie Bleves, Anne-Béatrice Blanc-Potard.

Supervision: Anne-Béatrice Blanc-Potard.

Validation: Preeti Garai, Anne-Béatrice Blanc-Potard.

Visualization: Preeti Garai, Malika Moussouni.

Writing – original draft: Preeti Garai, Anne-Béatrice Blanc-Potard.

Writing – review & editing: Preeti Garai, Laurence Berry, Malika Moussouni, Sophie Bleves, Anne-Béatrice Blanc-Potard.

References

1. Silva MT (2012) Classical labeling of bacterial pathogens according to their lifestyle in the host: inconsistencies and alternatives. Front Microbiol 3: 71. https://doi.org/10.3389/fmicb.2012.00071 PMID: 22393329
2. Pujol C, Bliska JB (2005) Turning Yersinia pathogenesis outside in: subversion of macrophage function by intracellular yersiniae. Clin Immunol 114: 216–226. https://doi.org/10.1016/j.clim.2004.07.013 PMID: 15721832
3. Kubica M, Guzik K, Koziel J, Zarebski M, Richter W, et al. (2008) A potential new pathway for *Staphylococcus aureus* dissemination: the silent survival of S. aureus phagocytosed by human monocyte-derived macrophages. PLoS One 3: e1409. https://doi.org/10.1371/journal.pone.0001409 PMID: 18183290
4. Garzoni C, Kelley WL (2009) *Staphylococcus aureus*: new evidence for intracellular persistence. Trends Microbiol 17: 59–65. https://doi.org/10.1016/j.tim.2008.11.005 PMID: 19208480
5. Flannagan RS, Heit B, Heinrichs DE (2016) Intracellular replication of *Staphylococcus aureus* in mature phagolysosomes in macrophages precedes host cell death, and bacterial escape and dissemination. Cell Microbiol 18: 514–535. https://doi.org/10.1111/cmi.12527 PMID: 26408990
6. Jubrail J, Morris P, Bewley MA, Stoneham S, Johnston SA, et al. (2016) Inability to sustain intraphagolysosomal killing of *Staphylococcus aureus* predisposes to bacterial persistence in macrophages. Cell Microbiol 18: 80–96. https://doi.org/10.1111/cmi.12485 PMID: 26248337
7. Ercoli G, Fernandes VE, Chung WY, Wanford JJ, Thomson S, et al. (2018) Intracellular replication of *Streptococcus pneumoniae* inside splenic macrophages serves as a reservoir for septicaemia. Nat Microbiol.
8. Klockgether J, Tummler B (2017) Recent advances in understanding *Pseudomonas aeruginosa* as a pathogen. F1000Res 6: 1261. https://doi.org/10.12688/f1000research.10506.1 PMID: 28794863
9. Engel J, Balachandran P (2009) Role of *Pseudomonas aeruginosa* type III effectors in disease. Curr Opin Microbiol 12: 61–66. https://doi.org/10.1016/j.mib.2008.12.007 PMID: 19168385
10. Hauser AR (2009) The type III secretion system of *Pseudomonas aeruginosa*: infection by injection. Nat Rev Microbiol 7: 654–665. https://doi.org/10.1038/nrmicro2199 PMID: 19680249
11. Feltman H, Schulert G, Khan S, Jain M, Peterson L, et al. (2001) Prevalence of type III secretion genes in clinical and environmental isolates of *Pseudomonas aeruginosa*. Microbiology 147: 2659–2669. https://doi.org/10.1099/00221287-147-10-2659 PMID: 11577145
12. Garcia-Medina R, Dunne WM, Singh PK, Brody SL (2005) *Pseudomonas aeruginosa* acquires biofilm-like properties within airway epithelial cells. Infect Immun 73: 8298–8305. https://doi.org/10.1128/IAI.73.12.8298-8305.2005 PMID: 16299327
13. Sana TG, Hachani A, Bucior I, Soscia C, Garvis S, et al. (2012) The second type VI secretion system of *Pseudomonas aeruginosa* strain PAO1 is regulated by quorum sensing and Fur and modulates internalization in epithelial cells. J Biol Chem 287: 27095–27105. https://doi.org/10.1074/jbc.M112.376368 PMID: 22665491
14. Mittal R, Grati M, Gerring R, Blackwelder P, Yan D, et al. (2014) *In vitro* interaction of *Pseudomonas aeruginosa* with human middle ear epithelial cells. PLoS One 9: e91885. https://doi.org/10.1371/journal.pone.0091885 PMID: 24632826
15. Kazmierczak BI, Jou TS, Mostov K, Engel JN (2001) Rho GTPase activity modulates *Pseudomonas aeruginosa* internalization by epithelial cells. Cell Microbiol 3: 85–98. PMID: 11207623
16. Angus AA, Lee AA, Augustin DK, Lee EJ, Evans DJ, et al. (2008) *Pseudomonas aeruginosa* induces membrane blebs in epithelial cells, which are utilized as a niche for intracellular replication and motility. Infect Immun 76: 1992–2001. https://doi.org/10.1128/IAI.01221-07 PMID: 18316391
17. Kroken AR, Chen CK, Evans DJ, Yahr TL, Fleiszig SMJ (2018) The Impact of ExoS on *Pseudomonas aeruginosa* Internalization by Epithelial Cells Is Independent of fleQ and Correlates with Bistability of Type Three Secretion System Gene Expression. MBio 9.
18. Angus AA, Evans DJ, Barbieri JT, Fleiszig SM (2010) The ADP-ribosylation domain of *Pseudomonas aeruginosa* ExoS is required for membrane bleb niche formation and bacterial survival within epithelial cells. Infect Immun 78: 4500–4510. https://doi.org/10.1128/IAI.00417-10 PMID: 20732998
19. Heimer SR, Evans DJ, Stern ME, Barbieri JT, Yahr T, et al. (2013) *Pseudomonas aeruginosa* utilizes the type III secreted toxin ExoS to avoid acidified compartments within epithelial cells. PLoS One 8: e73111. https://doi.org/10.1371/journal.pone.0073111 PMID: 24058462
20. Lovewell RR, Patankar YR, Berwin B (2014) Mechanisms of phagocytosis and host clearance of *Pseudomonas aeruginosa*. Am J Physiol Lung Cell Mol Physiol 306: L591–603. https://doi.org/10.1152/ajplung.00335.2013 PMID: 24464809

21. Brannon MK, Davis JM, Mathias JR, Hall CJ, Emerson JC, et al. (2009) *Pseudomonas aeruginosa* Type III secretion system interacts with phagocytes to modulate systemic infection of zebrafish embryos. Cell Microbiol 11: 755–768. https://doi.org/10.1111/j.1462-5822.2009.01288.x PMID: 19207728

22. Kumar SS, Tandberg JI, Penesyan A, Elbourne LDH, Suarez-Bosche N, et al. (2018) Dual Transcriptomics of Host-Pathogen Interaction of Cystic Fibrosis Isolate *Pseudomonas aeruginosa* PASS1 With Zebrafish. Front Cell Infect Microbiol 8: 406. https://doi.org/10.3389/fcimb.2018.00406 PMID: 30524971

23. Schmiedl A, Kerber-Momot T, Munder A, Pabst R, Tschernig T (2010) Bacterial distribution in lung parenchyma early after pulmonary infection with *Pseudomonas aeruginosa*. Cell Tissue Res 342: 67–73. https://doi.org/10.1007/s00441-010-1036-y PMID: 20838814

24. Buyck JM, Tulkens PM, Van Bambeke F (2013) Pharmacodynamic evaluation of the intracellular activity of antibiotics towards *Pseudomonas aeruginosa* PAO1 in a model of THP-1 human monocytes. Antimicrob Agents Chemother 57: 2310–2318. https://doi.org/10.1128/AAC.02609-12 PMID: 23478951

25. Belon C, Soscia C, Bernut A, Laubier A, Bleves S, et al. (2015) A Macrophage Subversion Factor Is Shared by Intracellular and Extracellular Pathogens. PLoS Pathog 11: e1004969. https://doi.org/10.1371/journal.ppat.1004969 PMID: 26080006

26. Mittal R, Lisi CV, Kumari H, Grati M, Blackwelder P, et al. (2016) Otopathogenic *Pseudomonas aeruginosa* Enters and Survives Inside Macrophages. Front Microbiol 7: 1828. https://doi.org/10.3389/fmicb.2016.01828 PMID: 27917157

27. Bernut A, Belon C, Soscia C, Bleves S, Blanc-Potard AB (2015) Intracellular phase for an extracellular bacterial pathogen: MgtC shows the way. Microb Cell 2: 353–355. https://doi.org/10.15698/mic2015.09.227 PMID: 28357311

28. Lee EJ, Pontes MH, Groisman EA (2013) A bacterial virulence protein promotes pathogenicity by inhibiting the bacterium's own F1Fo ATP synthase. Cell 154: 146–156. https://doi.org/10.1016/j.cell.2013.06.004 PMID: 23827679

29. Pontes MH, Lee EJ, Choi J, Groisman EA (2015) *Salmonella* promotes virulence by repressing cellulose production. Proc Natl Acad Sci U S A 112: 5183–5188. https://doi.org/10.1073/pnas.1500989112 PMID: 25848006

30. Alix E, Blanc-Potard AB (2007) MgtC: a key player in intramacrophage survival. Trends Microbiol 15: 252–256. https://doi.org/10.1016/j.tim.2007.03.007 PMID: 17416526

31. Belon C, Blanc-Potard AB (2016) Intramacrophage Survival for Extracellular Bacterial Pathogens: MgtC As a Key Adaptive Factor. Front Cell Infect Microbiol 6: 52. https://doi.org/10.3389/fcimb.2016.00052 PMID: 27242970

32. Fito-Boncompte L, Chapalain A, Bouffartigues E, Chaker H, Lesouhaitier O, et al. (2011) Full virulence of *Pseudomonas aeruginosa* requires OprF. Infect Immun 79: 1176–1186. https://doi.org/10.1128/IAI.00850-10 PMID: 21189321

33. Chevalier S, Bouffartigues E, Bodilis J, Maillot O, Lesouhaitier O, et al. (2017) Structure, function and regulation of *Pseudomonas aeruginosa* porins. FEMS Microbiol Rev 41: 698–722. https://doi.org/10.1093/femsre/fux020 PMID: 28981745

34. Bouffartigues E, Moscoso JA, Duchesne R, Rosay T, Fito-Boncompte L, et al. (2015) The absence of the *Pseudomonas aeruginosa* OprF protein leads to increased biofilm formation through variation in c-di-GMP level. Front Microbiol 6: 630. https://doi.org/10.3389/fmicb.2015.00630 PMID: 26157434

35. Ince D, Sutterwala FS, Yahr TL (2015) Secretion of Flagellar Proteins by the *Pseudomonas aeruginosa* Type III Secretion-Injectisome System. J Bacteriol 197: 2003–2011. https://doi.org/10.1128/JB.00030-15 PMID: 25845843

36. Soscia C, Hachani A, Bernadac A, Filloux A, Bleves S (2007) Cross talk between type III secretion and flagellar assembly systems in *Pseudomonas aeruginosa*. J Bacteriol 189: 3124–3132. https://doi.org/10.1128/JB.01677-06 PMID: 17307856

37. Moscoso JA, Mikkelsen H, Heeb S, Williams P, Filloux A (2011) The *Pseudomonas aeruginosa* sensor RetS switches type III and type VI secretion via c-di-GMP signalling. Environ Microbiol 13: 3128–3138. https://doi.org/10.1111/j.1462-2920.2011.02595.x PMID: 21955777

38. Rybtke MT, Borlee BR, Murakami K, Irie Y, Hentzer M, et al. (2012) Fluorescence-based reporter for gauging cyclic di-GMP levels in *Pseudomonas aeruginosa*. Appl Environ Microbiol 78: 5060–5069. https://doi.org/10.1128/AEM.00414-12 PMID: 22582064

39. Coburn J, Frank DW (1999) Macrophages and epithelial cells respond differently to the *Pseudomonas aeruginosa* type III secretion system. Infect Immun 67: 3151–3154. PMID: 10338535

40. Franchi L, Stoolman J, Kanneganti TD, Verma A, Ramphal R, et al. (2007) Critical role for Ipaf in *Pseudomonas aeruginosa*-induced caspase-1 activation. Eur J Immunol 37: 3030–3039. https://doi.org/10.1002/eji.200737532 PMID: 17935074

41. Galle M, Schotte P, Haegman M, Wullaert A, Yang HJ, et al. (2008) The *Pseudomonas aeruginosa* Type III secretion system plays a dual role in the regulation of caspase-1 mediated IL-1beta maturation. J Cell Mol Med 12: 1767–1776. https://doi.org/10.1111/j.1582-4934.2007.00190.x PMID: 18081695

42. Huber P, Bouillot S, Elsen S, Attree I (2014) Sequential inactivation of Rho GTPases and Lim kinase by *Pseudomonas aeruginosa* toxins ExoS and ExoT leads to endothelial monolayer breakdown. Cell Mol Life Sci 71: 1927–1941. https://doi.org/10.1007/s00018-013-1451-9 PMID: 23974244

43. Keller C, Mellouk N, Danckaert A, Simeone R, Brosch R, et al. (2013) Single cell measurements of vacuolar rupture caused by intracellular pathogens. J Vis Exp: e50116. https://doi.org/10.3791/50116 PMID: 23792688

44. Tsutsumi Y, Tomita H, Tanimoto K (2013) Identification of novel genes responsible for overexpression of *ampC* in *Pseudomonas aeruginosa* PAO1. Antimicrob Agents Chemother 57: 5987–5993. https://doi.org/10.1128/AAC.01291-13 PMID: 24041903

45. Hritonenko V, Evans DJ, Fleiszig SM (2012) Translocon-independent intracellular replication by *Pseudomonas aeruginosa* requires the ADP-ribosylation domain of ExoS. Microbes Infect 14: 1366–1373. https://doi.org/10.1016/j.micinf.2012.08.007 PMID: 22981600

46. Landeta C, Boyd D, Beckwith J (2018) Disulfide bond formation in prokaryotes. Nat Microbiol 3: 270–280. https://doi.org/10.1038/s41564-017-0106-2 PMID: 29463925

47. Vareechon C, Zmina SE, Karmakar M, Pearlman E, Rietsch A (2017) *Pseudomonas aeruginosa* Effector ExoS Inhibits ROS Production in Human Neutrophils. Cell Host Microbe 21: 611–618 e615. https://doi.org/10.1016/j.chom.2017.04.001 PMID: 28494242

48. Hauser AR, Engel JN (1999) *Pseudomonas aeruginosa* induces type-III-secretion-mediated apoptosis of macrophages and epithelial cells. Infect Immun 67: 5530–5537. PMID: 10496945

49. Dacheux D, Toussaint B, Richard M, Brochier G, Croize J, et al. (2000) *Pseudomonas aeruginosa* cystic fibrosis isolates induce rapid, type III secretion-dependent, but ExoU-independent, oncosis of macrophages and polymorphonuclear neutrophils. Infect Immun 68: 2916–2924. https://doi.org/10.1128/iai.68.5.2916-2924.2000 PMID: 10768989

50. Vance RE, Rietsch A, Mekalanos JJ (2005) Role of the type III secreted exoenzymes S, T, and Y in systemic spread of *Pseudomonas aeruginosa* PAO1 in vivo. Infect Immun 73: 1706–1713. https://doi.org/10.1128/IAI.73.3.1706-1713.2005 PMID: 15731071

51. Sutterwala FS, Mijares LA, Li L, Ogura Y, Kazmierczak BI, et al. (2007) Immune recognition of *Pseudomonas aeruginosa* mediated by the IPAF/NLRC4 inflammasome. J Exp Med 204: 3235–3245. https://doi.org/10.1084/jem.20071239 PMID: 18070936

52. Balakrishnan A, Karki R, Berwin B, Yamamoto M, Kanneganti TD (2018) Guanylate binding proteins facilitate caspase-11-dependent pyroptosis in response to type 3 secretion system-negative *Pseudomonas aeruginosa*. Cell Death Discov 5: 3.

53. Kaminski A, Gupta KH, Goldufsky JW, Lee HW, Gupta V, et al. (2018) *Pseudomonas aeruginosa* ExoS Induces Intrinsic Apoptosis in Target Host Cells in a Manner That is Dependent on its GAP Domain Activity. Sci Rep 8: 14047. https://doi.org/10.1038/s41598-018-32491-2 PMID: 30232373

54. Pederson KJ, Vallis AJ, Aktories K, Frank DW, Barbieri JT (1999) The amino-terminal domain of *Pseudomonas aeruginosa* ExoS disrupts actin filaments via small-molecular-weight GTP-binding proteins. Mol Microbiol 32: 393–401. PMID: 10231494

55. Wood SJ, Goldufsky JW, Bello D, Masood S, Shafikhani SH (2015) *Pseudomonas aeruginosa* ExoT Induces Mitochondrial Apoptosis in Target Host Cells in a Manner That Depends on Its GTPase-activating Protein (GAP) Domain Activity. J Biol Chem 290: 29063–29073. https://doi.org/10.1074/jbc.M115.689950 PMID: 26451042

56. Sawa T, Shimizu M, Moriyama K, Wiener-Kronish JP (2014) Association between *Pseudomonas aeruginosa* type III secretion, antibiotic resistance, and clinical outcome: a review. Crit Care 18: 668. https://doi.org/10.1186/s13054-014-0668-9 PMID: 25672496

57. Munzenmayer L, Geiger T, Daiber E, Schulte B, Autenrieth SE, et al. (2016) Influence of Sae-regulated and Agr-regulated factors on the escape of *Staphylococcus aureus* from human macrophages. Cell Microbiol 18: 1172–1183. https://doi.org/10.1111/cmi.12577 PMID: 26895738

58. Rang C, Alix E, Felix C, Heitz A, Tasse L, et al. (2007) Dual role of the MgtC virulence factor in host and non-host environments. Mol Microbiol 63: 605–622. https://doi.org/10.1111/j.1365-2958.2006.05542.x PMID: 17176255

59. Nivens DE, Ohman DE, Williams J, Franklin MJ (2001) Role of alginate and its O acetylation in formation of *Pseudomonas aeruginosa* microcolonies and biofilms. J Bacteriol 183: 1047–1057. https://doi.org/10.1128/JB.183.3.1047-1057.2001 PMID: 11208804

60. Bessoles S, Dudal S, Besra GS, Sanchez F, Lafont V (2009) Human CD4+ invariant NKT cells are involved in antibacterial immunity against *Brucella suis* through CD1d-dependent but CD4-independent mechanisms. Eur J Immunol 39: 1025–1035. https://doi.org/10.1002/eji.200838929 PMID: 19266487

61. Gannoun-Zaki L, Alibaud L, Carrere-Kremer S, Kremer L, Blanc-Potard AB (2013) Overexpression of the KdpF membrane peptide in *Mycobacterium bovis* BCG results in reduced intramacrophage growth and altered cording morphology. PLoS One 8: e60379. https://doi.org/10.1371/journal.pone.0060379 PMID: 23577107

62. Martinez E, Allombert J, Cantet F, Lakhani A, Yandrapalli N, et al. (2016) *Coxiella burnetii* effector CvpB modulates phosphoinositide metabolism for optimal vacuole development. Proc Natl Acad Sci U S A 113: E3260–3269. https://doi.org/10.1073/pnas.1522811113 PMID: 27226300